PB99-100125

REPORT FHWA/NY/RR-93/159

Load Testing, Finite Element Analysis, And Design of Steel Traffic-Signal Poles

SHERIF J. BOULOS
GONGKANG FU
SREENIVAS ALAMPALLI

RESEARCH REPORT 159

ENGINEERING RESEARCH AND DEVELOPMENT BUREAU
NEW YORK STATE DEPARTMENT OF TRANSPORTATION
Mario M. Cuomo, Governor/John C. Egan, Commissioner

STATE OF NEW YORK

Mario M. Cuomo, Governor

DEPARTMENT OF TRANSPORTATION

John C. Egan, Commissioner
Michael J. Cuddy, Assistant Commissioner for Engineering and Chief Engineer
Paul J. Mack, Deputy Chief Engineer, Technical Services Division
Robert J. Perry, Director of Engineering Research and Development

The Engineering Research and Development Bureau conducts and manages the engineering research program of the New York State Department of Transportation. The Federal Highway Administration provides financial and technical assistance for these research activities, including review and approval of publications.

Contents of research publications are reviewed by the Bureau's Director, and the appropriate section head. However, these publications primarily reflect the views of their authors, who are responsible for correct use of brand names and for the accuracy, analysis, and inferences drawn from the data.

It is the intent of the New York State Department of Transportation and the Federal Highway Administration that research publications not be used for promotional purposes. This publication does not endorse or approve any commercial product even though trade names may be cited, does not necessarily reflect official view or policies of either agency and does not constitute a standard, specification, or regulation.

ENGINEERING RESEARCH PUBLICATIONS

A. D. Emerich, Editor
Donna L. Noonan, Graphics and Production
Nancy A. Troxell and Jeanette M. LaClair, Copy Preparation

LOAD TESTING, FINITE ELEMENT ANALYSIS, AND DESIGN OF STEEL TRAFFIC-SIGNAL POLES

Sherif J. Boulos, Civil Engineer I
Gongkang Fu, Engineering Research Specialist II
Sreenivas Alampalli, Engineering Research Specialist I

Final Report on Research Project 12-29
Conducted in Cooperation With
The U.S. Department of Transportation
Federal Highway Administration

Research Report 159
July 1993

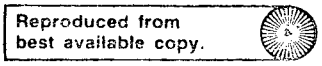

ENGINEERING RESEARCH AND DEVELOPMENT BUREAU
New York State Department of Transportation
State Campus, Albany, New York 12232

TECHNICAL REPORT STANDARD TITLE PAGE

1. Report No.		3. Recipient's Catalog No.
FHWA/NY/RR-93/159	PB99-100125	

4. Title and Subtitle	5. Report Date
LOAD TESTING, FINITE ELEMENT ANALYSIS, AND DESIGN OF STEEL TRAFFIC-SIGNAL POLES	July 1993
	6. Performing Organization Code
7. Author(s)	8. Performing Organization Report No.
Sherif J. Boulos, Gongkang Fu, and Sreenivas Alampalli	Research Report 159
9. Performing Organization Name and Address	10. Work Unit No.
Engineering Research and Development Bureau New York State Department of Transportation State Campus, Albany, New York 12232	11. Contract or Grant No.
	13. Type of Report and Period Covered
12. Sponsoring Agency Name and Address	Final Report Research Project 12-29
Offices of Research, Development & Technology HRD-10 Federal Highway Administration U.S. Department of Transportation Washington, DC 20590	14. Sponsoring Agency Code

15. Supplementary Notes

Prepared in cooperation with the U.S. Department of Transportation, Federal Highway Administration. Study Title: Analysis and Design of Span-Wire Traffic-Signal Poles.

16. Abstract

At request of the Structures Design and Construction Division, the Engineering Research and Development Bureau performed full-scale testing and finite element analysis (FEA) of span-wire traffic-signal poles to evaluate their structural adequacy. Results of testing and analysis of four poles indicated that they were structurally inadequate. The supporting base plate and anchor bolts were found to be the deficient components, but the pole's post was adequately designed. FEA models of the signal poles verified by the test results were then used to evaluate a representative sample of poles from three major suppliers to New York State. Evaluation criteria were based on adequacy of the base plate and anchor bolts. Results showed that plates designed by the manufacturers' current methods were not adequate to carry the design loads. Thus, a new design method for the base plate has been developed, based on results of the tests and analyses. This method is simple for routine applications, and consistent with the current AASHTO code. The anchor bolts were also found deficient with respect to axial capacity, apparently due to neglecting a critical (diagonal) load case, and this load must be considered in design.

17. Key Words	18. Distribution Statement
traffic signal poles, finite element analysis, testing, base plates, anchor bolts, design	No restrictions. This document is available to the public through the National Technical Information Service, Springfield VA 22161

19. Security Classif. (of this report)	20. Security Classif. (of this page)	21. No. of Pages	22. Price
Unclassified	Unclassified	vi + 53	

Form DOT F 1700.7 (8-69)

Preceding page blank

METRIC (SI*) CONVERSION FACTORS

APPROXIMATE CONVERSIONS TO SI UNITS

Symbol	When You Know	Multiply By	To Find	Symbol
LENGTH				
in	inches	2.54	millimetres	mm
ft	feet	0.3048	metres	m
yd	yards	0.914	metres	m
mi	miles	1.61	kilometres	km
AREA				
in²	square inches	645.2	millimetres squared	mm²
ft²	square feet	0.0929	metres squared	m²
yd²	square yards	0.836	metres squared	m²
mi²	square miles	2.59	kilometres squared	km²
ac	acres	0.395	hectares	ha
MASS (weight)				
oz	ounces	28.35	grams	g
lb	pounds	0.454	kilograms	kg
T	short tons (2000 lb)	0.907	megagrams	Mg
VOLUME				
fl oz	fluid ounces	29.57	millilitres	mL
gal	gallons	3.785	litres	L
ft³	cubic feet	0.0328	metres cubed	m³
yd³	cubic yards	0.0765	metres cubed	m³

NOTE: Volumes greater than 1000 L shall be shown in m³.

TEMPERATURE (exact)

°F	Fahrenheit temperature	5/9 (after subtracting 32)	Celsius temperature	°C

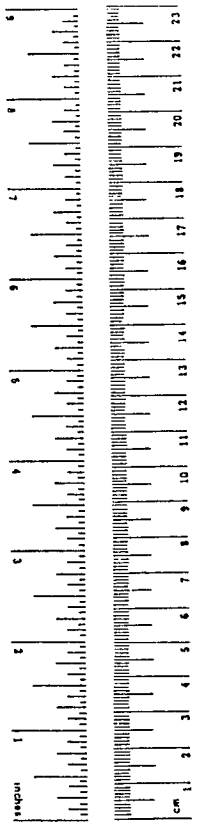

APPROXIMATE CONVERSIONS TO SI UNITS

Symbol	When You Know	Multiply By	To Find	Symbol
LENGTH				
mm	millimetres	0.039	inches	in
m	metres	3.28	feet	ft
m	metres	1.09	yards	yd
km	kilometres	0.621	miles	mi
AREA				
mm²	millimetres squared	0.0016	square inches	in²
m²	metres squared	10.764	square feet	ft²
km²	kilometres squared	0.39	square miles	mi²
ha	hectores (10 000 m²)	2.53	acres	ac
MASS (weight)				
g	grams	0.0353	ounces	oz
kg	kilograms	2.205	pounds	lb
Mg	megagrams (1 000 kg)	1.103	short tons	T
VOLUME				
mL	millilitres	0.034	fluid ounces	fl oz
L	litres	0.264	gallons	gal
m³	metres cubed	35.315	cubic feet	ft³
m³	metres cubed	1.308	cubic yards	yd³

TEMPERATURE (exact)

°C	Celsius temperature	9/5 (then add 32)	Fahrenheit temperature	°F

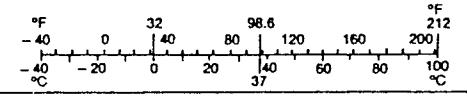

These factors conform to the requirement of FHWA Order 5190.1A.

* SI is the symbol for the International System of Measurements

CONTENTS

Figure 1. Typical traffic signal pole details.

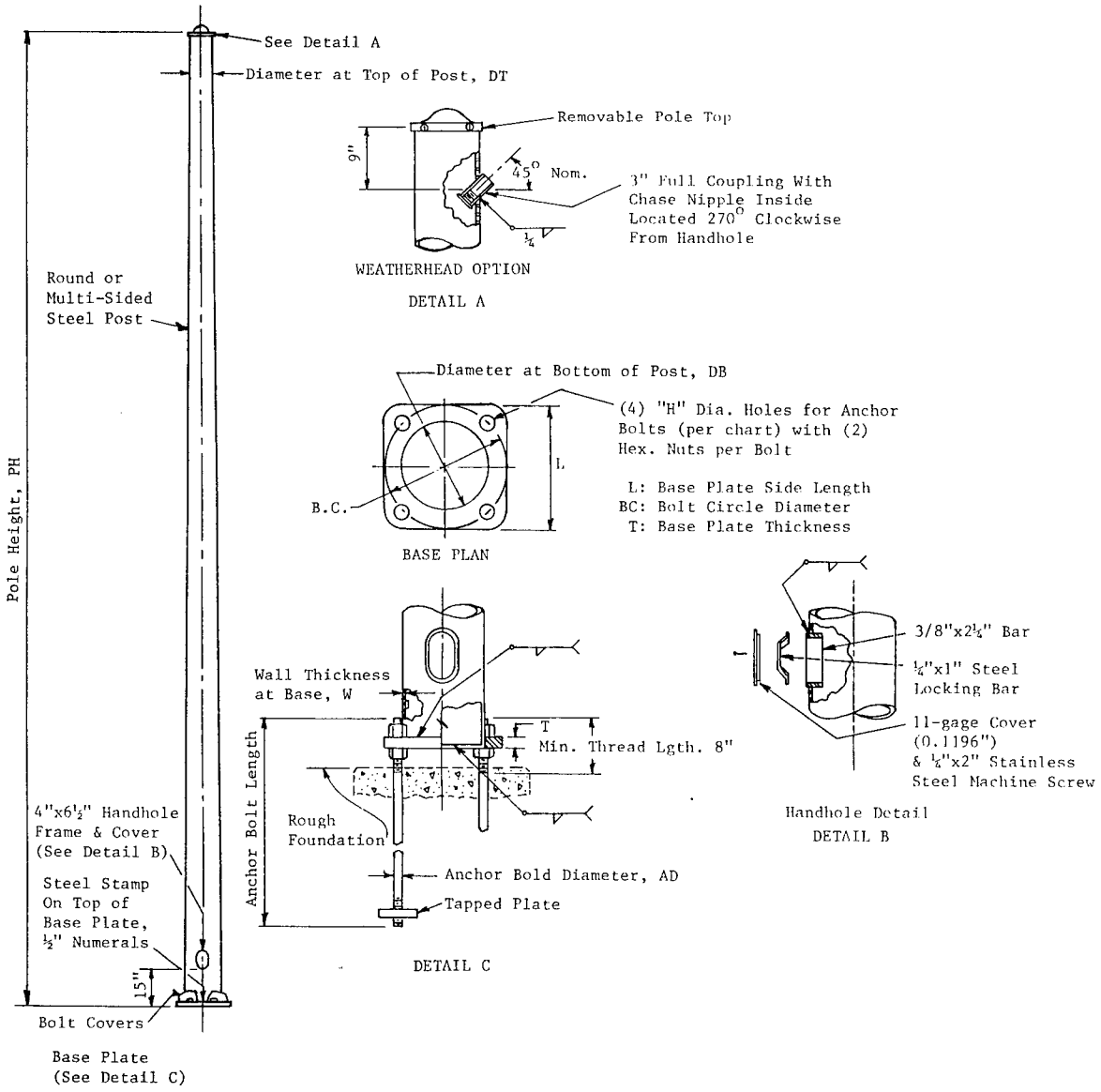

Figure 2. Span wire-mounted traffic signals and supporting poles.

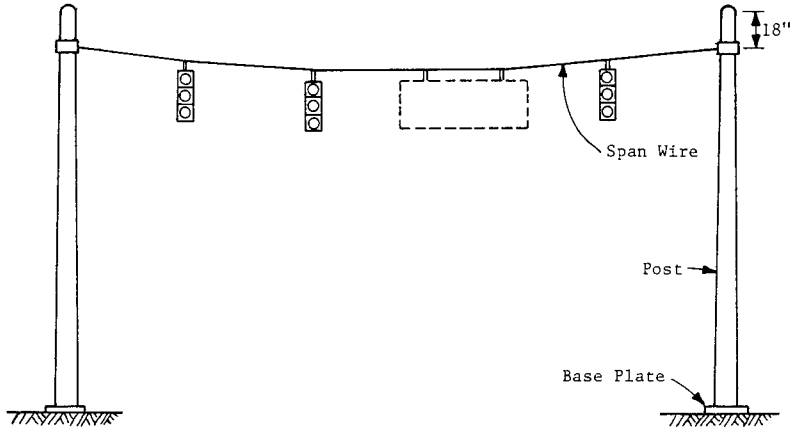

I. INTRODUCTION

A. Background

At request of the Structures Design and Construction Division, the study reported here was initiated to investigate structural adequacy of poles for span-wire-mounted traffic signals in New York State. Those in use had been designed by their manufacturers, and their adequacy was questioned by the Structures Division. Validity of design methods for the pole's base plate was of particular concern, although no incident of structural failure of such poles in service had been reported, except an accident when a truck snagged the wire mounted between two such poles.

A typical pole is composed of a round or polygonal steel post of changing diameter(s), welded to a square steel base plate. The plate is anchored to a concrete footing by four bolts. Each anchor bolt is tied to the base plate by two hexagonal nuts. A 4-by 6.5-in. reinforced hand hole is provided in the post 15 in. above the base plate. Typical pole details are shown in Figure 1. Typically two poles hold a span wire as shown in Figure 2. This wire, carrying traffic signals, is connected to the post 18 in. below its top. The wire is post-tensioned after the signals are mounted to reduce sag due to dead load, and sag is set to 5 percent of the span. Poles discussed in this report are designated by the first letter of their manufacturer's name, their design load in kips, and their height in feet. For example, C530 is a pole manufactured by the Carlan Manufacturing Company, with a design load of 5 kips, and 30 ft tall; S1036 is manufactured by Summit Manufacturing Inc., designed for a load of 10 kips, and 36 ft tall.

A concentrated horizontal force acting at 18 in. from top of pole (at the attachment point of the wire) is used as its design load. This load is calculated according to Engineering Instruction 83-38 (1), which in turn is based on the current AASHTO specification (2). Wire forces due to dead load, wind load, and ice load are calculated and combined into the following groups: I: dead load (for 100 percent of allowable stress), II: dead load plus wind (for 140 percent of allowable stress), and III: dead load plus ice load plus 1/2 wind (for 140 percent of allowable stress). Dead load is due to weights of the mounted signals, and ice and wind loads -- depending on the zone where the pole is erected (2). The group producing the highest stress ratio is used as the critical load group. Typically, Group II or Group III loading governs pole strength design in New York. For given loads, the force obtained from the critical load group is increased to the next larger 1000-lb increment, and selected as the pole's design load. Design stresses for Group II and Group III loads are 140 percent of the corresponding allowable stress units for steel. For example, allowable bending stress for steel plates is $0.66F_y$ and corresponding design stress for bending equals $1.4 \times 0.66\ F_y = 0.924\ F_y$, where F_y is nominal

Figure 3. Critical orientations of span wire with respect to base plate.

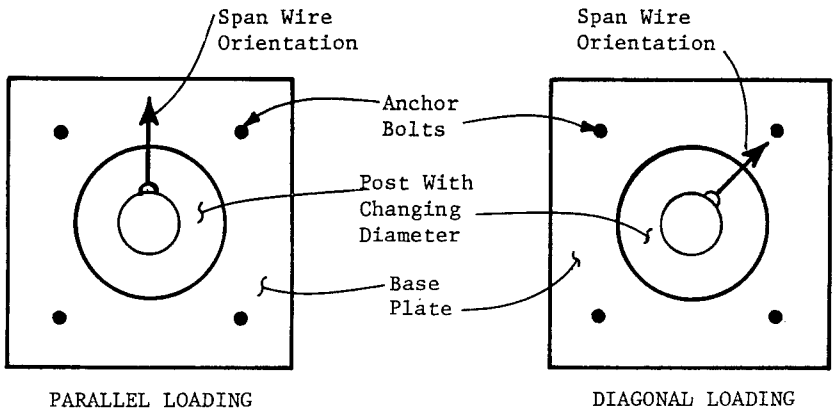

yield stress of the steel used. The AASHTO specification (2) provides guidelines to analyze the post as a cantilever according to the beam theory, and to design the anchor bolts to carry axial and shear forces. However, no particular method is specified for analysis of the base plate.

Two cases of loading are identified here as critical to the poles, depending on orientation of the span wire with respect to the base plate, as shown in Figure 3: 1) parallel loading where the wire runs parallel to a side of the square base plate, and 2) diagonal loading where the wire runs along a diagonal of the base plate. Thus, this study considered these two cases of loading in both testing and analysis.

B. Objectives and Approach

Objectives of this study were: 1) to examine structural behavior of signal poles under loads in critical orientations, 2) to determine structural adequacy of the poles and extent of deficiencies, if any, with respect to integrity of their individual components (post, hand hole, base plate, and anchor bolts), and 3) to develop a rational method to design signal poles, should current methods prove unreliable. Four full-scale poles were load tested, three of them instrumented with electrical-resistance strain gages. Their steel strengths were obtained by lab testing. Strength of the poles was assessed by their deflection and strain/stress behavior under loads. The test results were also used to verify a three-dimensional finite-element model that was developed for analysis. This verified model was then generalized to analyze and evaluate poles supplied to New York State by various manufacturers. Based on the results of these load tests and finite element analysis (FEA), a method was developed for designing signal poles.

II. FULL-SCALE TESTING

Full-scale testing of the signal poles was considered the most reliable means to study their structural behavior and determine their adequacy. The testing was also essential to verify the finite-element model developed to analyze representative sample poles. This chapter describes the tested poles, test setup and instrumentation, and test procedures, and discusses the test results.

A. Tested Poles

Four poles were selected for testing after consultation with the Structures Division. They were designed and fabricated by Carlan Manufacturing Company. Three were from Carlan's standard stock: C326, C530, and C832. The fourth (C530(T)) was specially built with a thinner (1.25-in. thick) base plate (vs. 1.75 in. for the standard C530 pole) to examine the effect of plate thickness on stress levels. Dimensions of tested poles are given in Table 1. They were selected to include different base plate thicknesses, and various clearances between bolt circle diameter (BC) and pole diameter at the bottom (DB). These two parameters were initially considered important factors affecting stress distribution in the base plate.

B. Test Setup and Instrumentation

All poles tested were anchored horizontally to a 3-in. thick steel foundation secured to a concrete block foundation extending 20 ft below ground. Loads were applied vertically upward to the poles 18 in. from their tips by a hydraulic jack. The jack was placed on a steel plate 3/4-in. thick and about 16 sq. ft in area resting on the ground. Test setup details and a mounted pole are shown in Figure 4.

Table 1. Dimension details of tested signal poles.

Pole ID	C326	C530 and C530(T)	C832
Pole Height PH, ft	26	30	32
Design Load, kips	3	5	8
Diameter at Top of Post DT, in.	8.625	10.75	12.75
Diameter at Bottom of Post DB, in.	10.75	12.75	16
Wall Thickness of Post at Base f_w, in.	0.25	0.313	0.375
Base Plate Side Length L, in.	17	23	22
Base Plate Thickness T, in.	1.5	1.75(1.25)*	2.25
Bolt Circle Diamer BC, in.	17	23	22
Anchor Bolt Diameter AD, in.	1.25	1.5	2.0

*C530(T) thickness in parenthesis.

Figure 4. Typical setup details (not to scale) and views of mounted test pole.

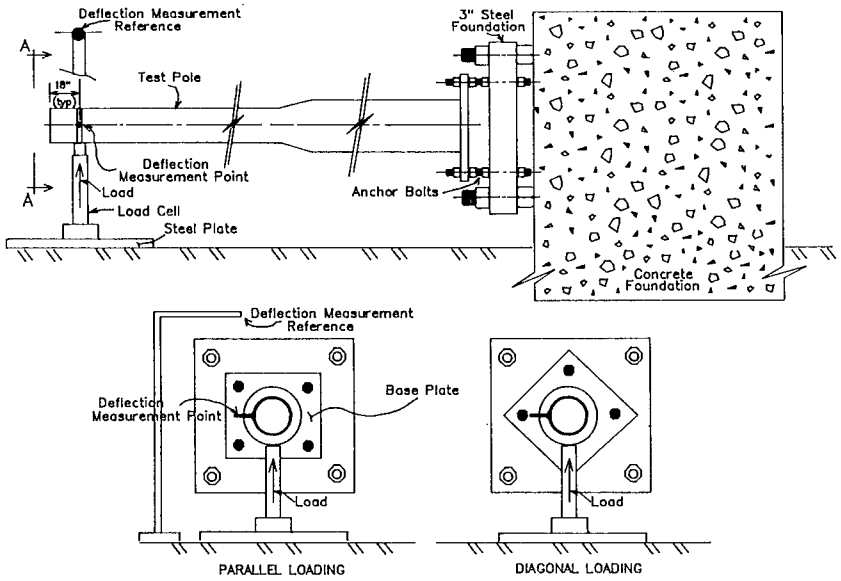

View A–A

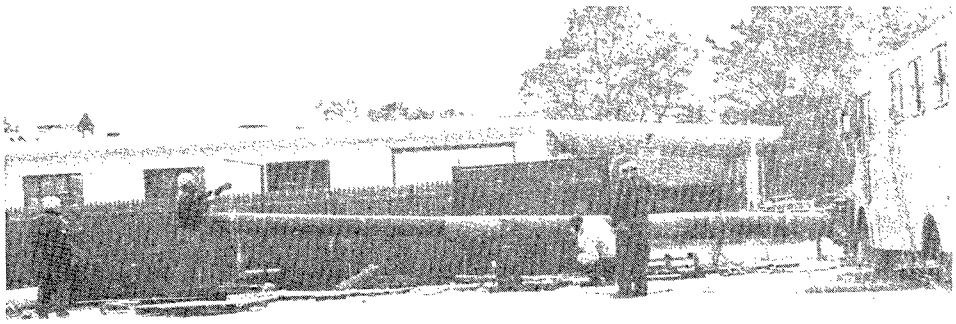

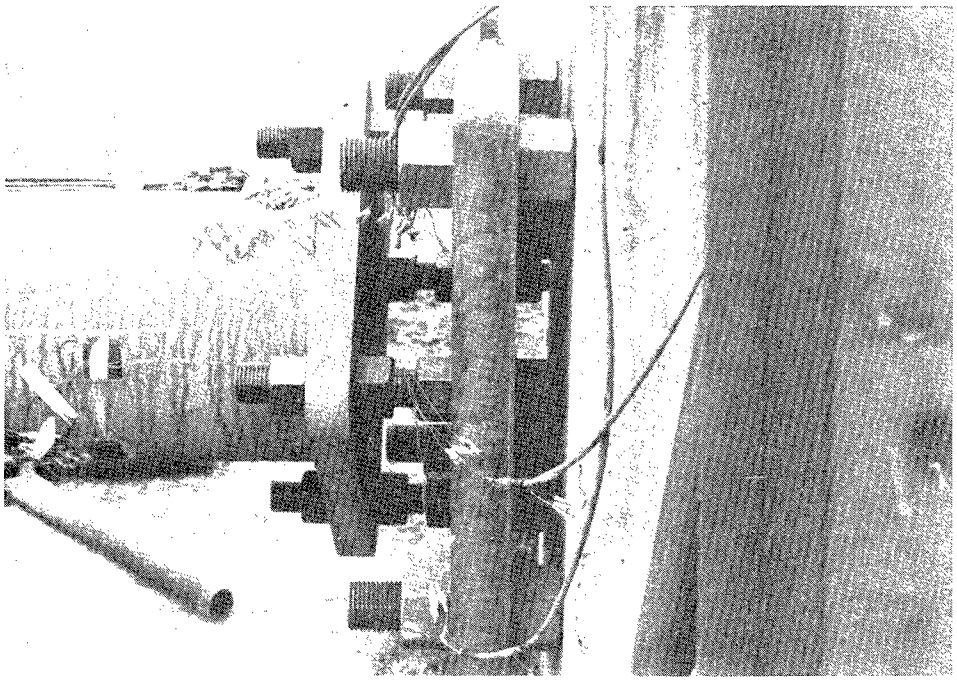

Levels of applied load were measured by a pressure gage with a resolution of 223.6 lb (100 psi on a cylinder area of 2.236 sq. in.). Appendix A gives details of the loading jack specifications. Each pole was subjected to either diagonal or parallel loading by rotating it about its central axis without changing the direction of the load (Fig. 4). Each tested pole required an anchor foundation matching its anchor bolt size and bolt circle. No concrete packing was provided between the pole's base plate and the steel test foundation (Fig. 4), as might be the case in a service condition. A suspended steel bar was fixed above the free end of the test pole as a measurement reference for the pole's tip deflection. Deflection was measured with a regular measuring tape with a resolution of 1/16 in. These details are also shown in Figure 4.

Electrical resistance self-temperature-compensating strain gages of a single arm or three arms were used to obtain strains/stresses of the poles (Appendix B). Location and orientation of each gage installed on the test poles were determined based on results of a preliminary FEA. Three poles (C530, C832, and C530(T)) were instrumented with electrical-resistance strain gages on the post, base plate, and anchor bolts. Table 2 and Figures 5, 6, and 7 give strain gage identifications and locations on the instrumented poles.

The strain gages were installed after thoroughly grinding and cleaning the target areas. To install the gages on the anchor bolts, threads were ground off in the target areas for a smooth surface. Accordingly, actual net area and section modulus of the anchors were reduced at the instrumented sections. An FX static data acquisition system was used to acquire strain data from the gages.

C. Material and Load Test Program and Results

A total of six load tests were performed on the selected poles. Each started with recording an initial tip position, and strain gage readings (if applicable) after the test pole was anchored to the foundation and before loading. The effect of the pole's dead weight on deflections and strains/stresses could thus be eliminated from later readings due to applied loads. The jack load was applied in increments and cycled up to the nominal design load or apparent yield (failure). Strain gage readings were used to assess adequacy of the pole's individual components, and to verify the FEA models. Note that, for simplicity of presentation, structural response obtained in strain has been converted here to stress according to the elastic stress/strain constitutive relation (see Appendix B for more details).

At each increment of loading tip displacement and strain gage readings were recorded. A load-tip deflection curve, showing the load cycles, was plotted for each test. Yielding was then identified as significant slope change of the curve with its corresponding applied load recognized as yielding load or strength of the pole. Since the pole's dead load was acting in the opposite direction from that of the applied load, actual yielding load should be lower than the observed applied load. In other words, yielding load obtained as described is conservatively an overestimation of real yielding load.

Figure 5. Strain gage details of Pole C530(T) (Test 2).

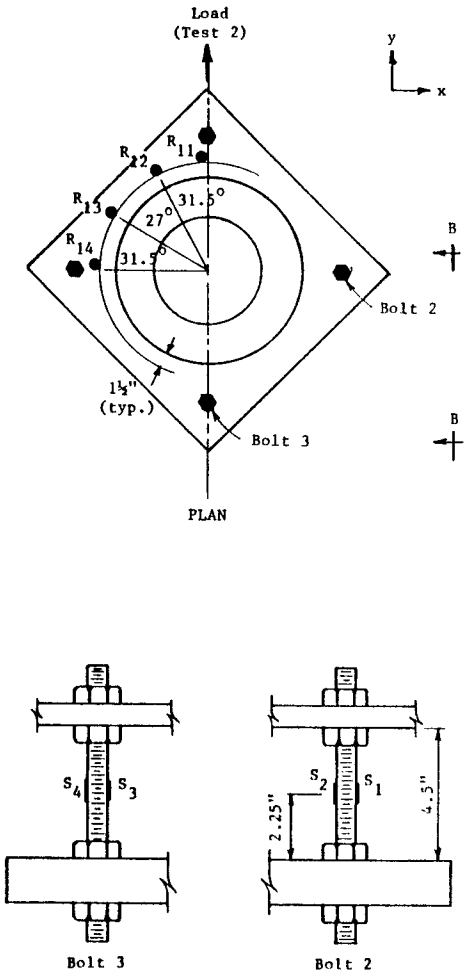

Figure 6. Strain gage details of Pole C530 (Tests 3 and 4).

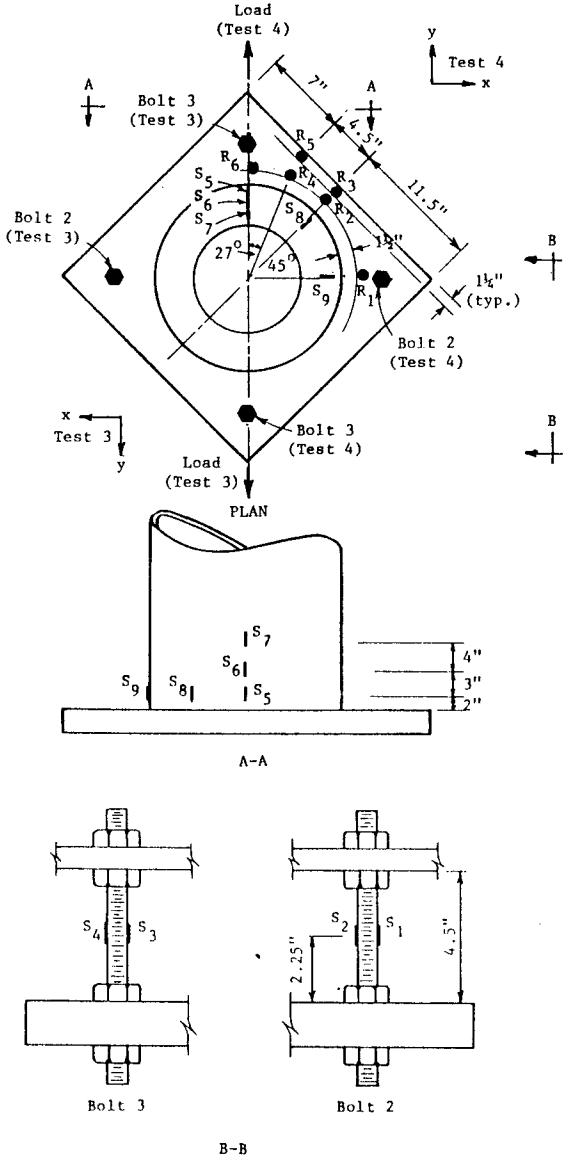

Figure 7. Strain gage details of Pole C832 (Tests 5 and 6).

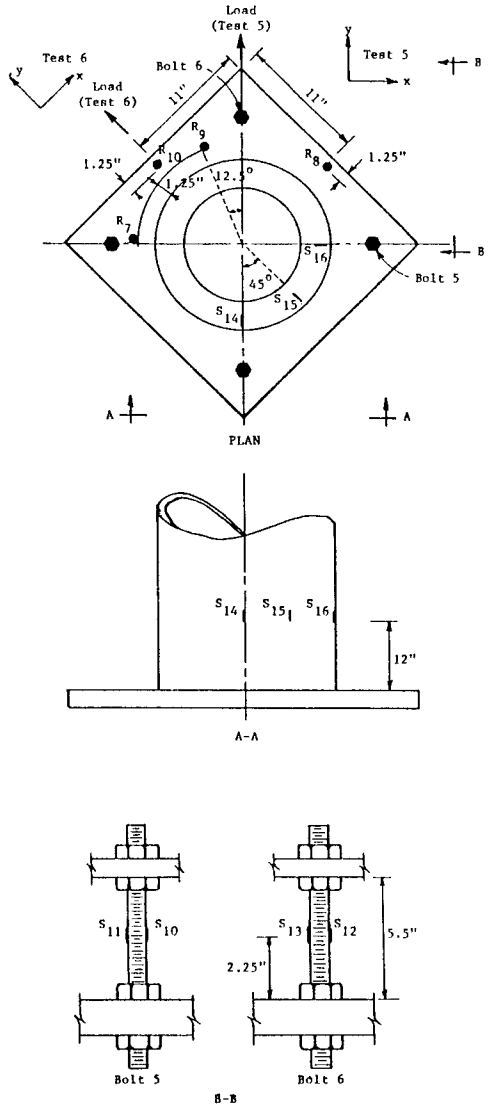

Table 2. Details of strain gages on instrumented poles.

Gage ID*	Location	Measurement Purpose
A. Strain Gages on Pole C530(T) (Fig. 5)		
S1,S2	On Bolt 2	Axial stress in bolt
S3,S4	On Bolt 3	Axial and bending stresses in bolt
R11 to R14	On top surface of base plate	Principal stresses in base plate
B. Strain Gages on Pole C530 (Fig. 6)		
S1,S2**	On Bolt 2	Axial stress in bolt
S3,S4**	On Bolt 3	Axial and bending stresses in bolt
S5 to S9	On post outer surface near base plate	Bending stresses in post
R1 to R6	On top surface of base plate	Principal stresses in base plate
C. Strain Gages on Pole C832 (Fig. 7)		
S10 to S13	On Bolts 5 and 6	Axial and bending stresses in bolts
S14 to S16	At post outer surface near base plate	Bending stresses in post
R7 to R10	On top surface of base plate	Principal stresses in base plate

*S = single-arm gage, R = three-arm rosette.
**Same anchor bolts were used for C530(T) and C530.

Table 3. Materials coupon test results.

Pole ID	Sample Source	Steel Type	Nominal Yield, ksi	0.2% Yield, ksi	Ultimate Strength, ksi
C326	Post	A53	50	57.0	71.8
	Plate	A36	36	42.7	69.0
	Bolt	A36M55	55	64.0	90.1
C530	Post	A252	50	54.4	71.1
	Plate	A36	36	37.1	63.2
	Bolt	A36M55	55	60.5	88.6
C832	Post	A53	50	47.3	70.9
	Plate	A36	36	28.2	44.9
	Plate*	A36	36	29.0*	44.1*
	Bolt	A36M55	55	58.8	86.3

*Second sample tested for verification.

1. Materials Tests

Upon conclusion of the load tests, samples were taken from each load-tested standard pole's post, base plate, and anchor bolts for lab test by the Materials Bureau. Table 3 shows material coupon test results. All tensile tests were performed according to ASTM Standard A 370 using a 30,000-lb load range and 2-percent pre/post-yield strain range. True yield strengths are listed with their corresponding nominal values. A second sample from the C832 base plate was tested to verify the first test, which had shown an unexpectedly low strength.

Figure 8. Load Test 1: Pole C326 under diagonal load.

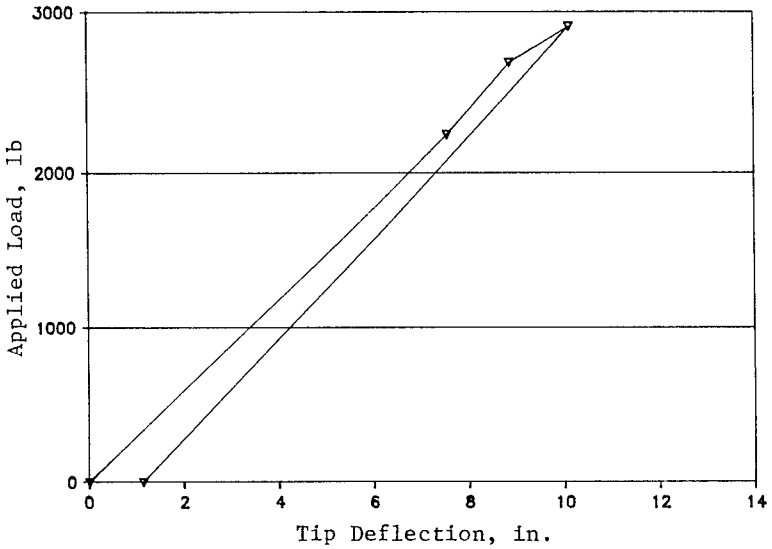

2. Load Tests

a. Load Test 1

Pole C326 was loaded diagonally to failure (with no strain gages) to allow the test crew to familiarize themselves with the test procedure and hardware. Only deflection was recorded. The resulting load-deflection curve is shown in Figure 8. As noted by the curve's significant slope change, the pole yielded at an applied load between 2683 and 2907 lb, which was lower than the design load of 3000 lb. Since the actual yield load is lower than this load (due to the dead load's opposite action, as noted earlier), the pole was considered inadequate.

b. Load Test 2

Pole C530(T) was instrumented and loaded diagonally to failure. Its instrumentation is shown in Figure 5. Two load cycles were applied, the first up to a load of 4025 lb and the second to 4616 lb. Figure 9a shows load-deflection cycles for this test. It is observed that more than 1 and 5 in. of residual displacements resulted from these successive loading cycles. They indicated the pole's failure (yield) under an applied load between 2460 and 3130 lb.

Figures 9b, 9c, and 9d exhibit responses of structural components to the loads, in terms of stress. Figure 9b shows that Anchor Bolt 3 (Gage S3) experienced a stress level of 69.0 ksi, high enough to cause material yielding under a load as low as 2460 lb. Note that axial stress (due to axial force) is much lower, as shown by average values of S3 and S4 readings in Figure 9b. Under the same load, Gage R12 in Figure 9d

Figure 9. Load Test 2: Pole C530(T) under diagonal load.

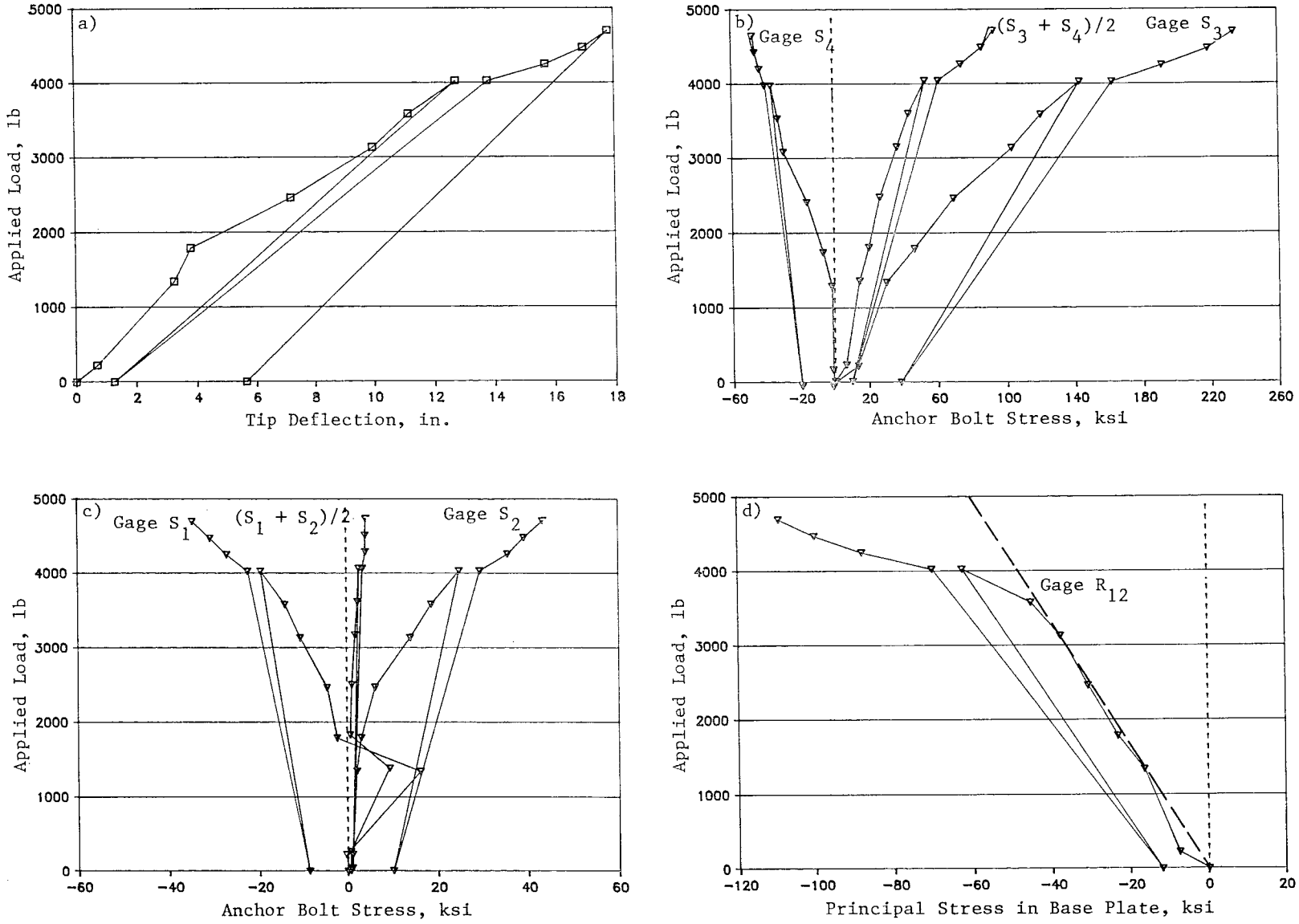

experienced a principal stress of 30.8 ksi in the base plate. It follows from these observations that this pole failed under the applied load of 2460 lb, due to initiation of yielding in an anchor bolt. In addition, by linear extrapolation of the first (elastic) part of the stress-load relation of Figure 9d in a broken line, the base plate is also a deficient component of the pole. It was observed that at the end of test, the base plate was permanently bent in the area between Gages R12 and R13 (see Fig. 5 for their location), as well as its symmetric counterpart. Although some experimental errors were observed (e.g., stress of S1 at 1342-lb load in Fig. 9c), the strain gage and deflection readings sufficiently demonstrated the pole's behavior under loading.

c. Load Test 3

Pole C530 was subjected to diagonal loading with strain gages on the post observing tensile strain (Table 2 and Fig. 6). The same anchor bolts used in Test 2 were used here. The pole was loaded successively up to 2460 and 2907 lb in two cycles. The load-deflection curve of this test is shown in Figure 10a. Applied loads were intentionally kept low to prevent the pole from yielding, so no yield was observed (Fig. 10).

Also, linear extrapolation of the demonstrated behaviors in these figures provides more insights. Among strain gages on the base plate, R4 showed the highest stress level under the loads. For example, maximum principal stress at R4 due to 2460-lb load was 22.2 ksi, as shown in Figure 10d. By simple linear extrapolation, this stress would reach 33.3 ksi (0.924 F_y) at 3369 lb -- 26 percent lower than the pole's design capacity of 5000 lb. This indicates deficiency of the base plate. This is also true for Anchor Bolt 3 with respect to axial stress (average of S3 and S4 in Fig. 10b).

d. Load Test 4

In this test, Pole C530 from Load Test 3 was reset for diagonal loading by turning the pole 180 deg about its central axis, with strain gages on the post experiencing compressive strain (Table 2 and Fig. 6). This was done to verify assumed symmetric behavior of the pole under applied loads. Three successive load cycles were carried out: 2460, 2907, and 4025 lb. Comparison of results in the linear range from Test 3 and this test verified the assumed symmetry.

Figure 11a shows the load-deflection curve for this test -- the pole behaved linearly up to a load of 3354 lb. Tensile stress of an outer fiber in Anchor Bolt 3 under this load was much higher than its actual and nominal yield stresses (60.5 and 55 ksi, respectively) as shown in Figure 11b, indicating that yielding began. Axial stress due to tensile force (average of Gages S3 and S4 in Fig. 11b) shows by linear extrapolation that this anchor bolt could not carry the 5000-lb design load due to excessive stress. Figure 11d demonstrates principal stress of Gage R4 on the base plate under the loads. At the same load of 3354 lb where elastic behavior was confirmed, R4 had stress as high as 28.8 ksi. Linear

Figure 10. Load Test 3: Pole C530 under Diagonal Load I.

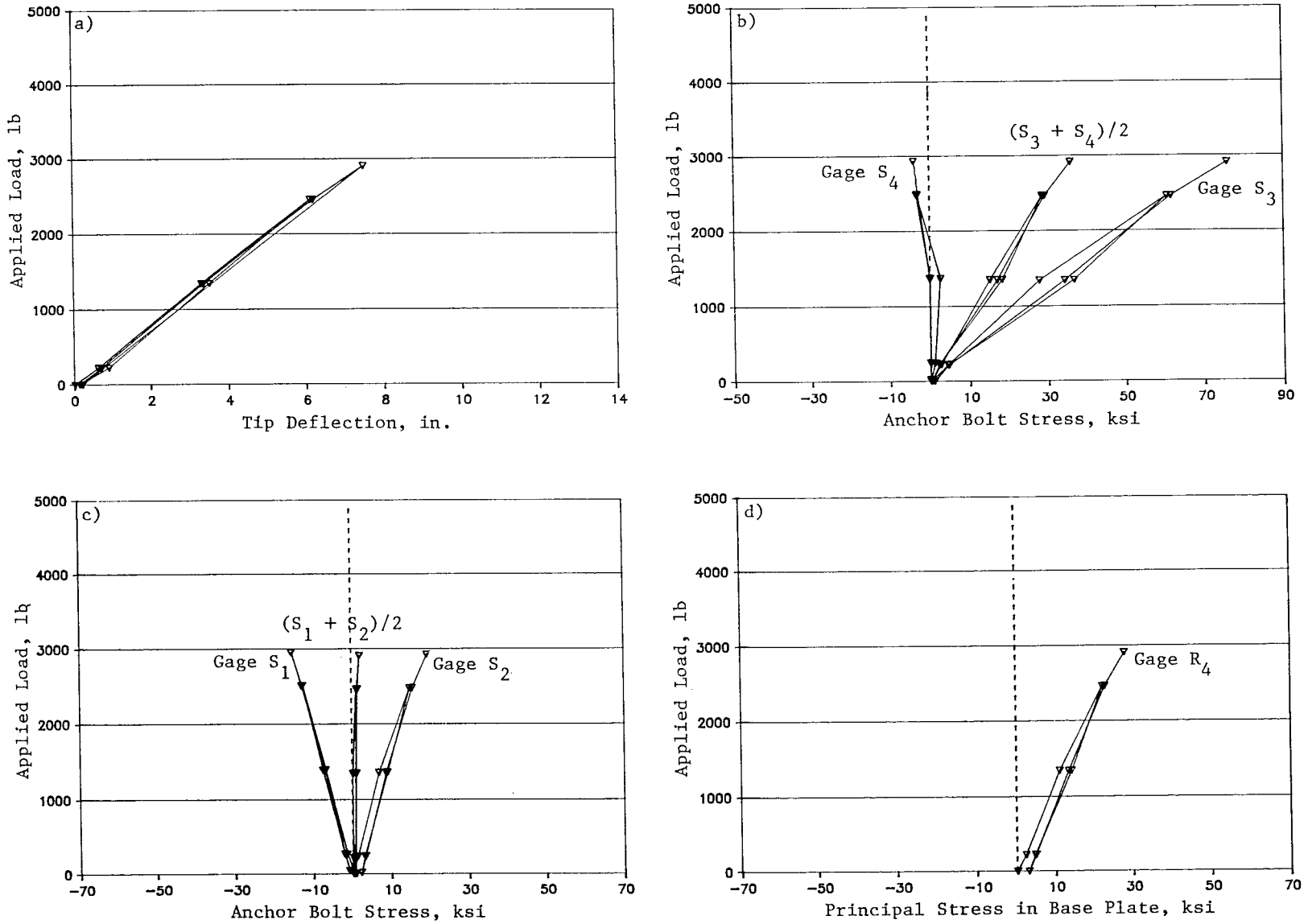

Figure 11. Load Test 4: Pole C530 under Diagonal Load II.

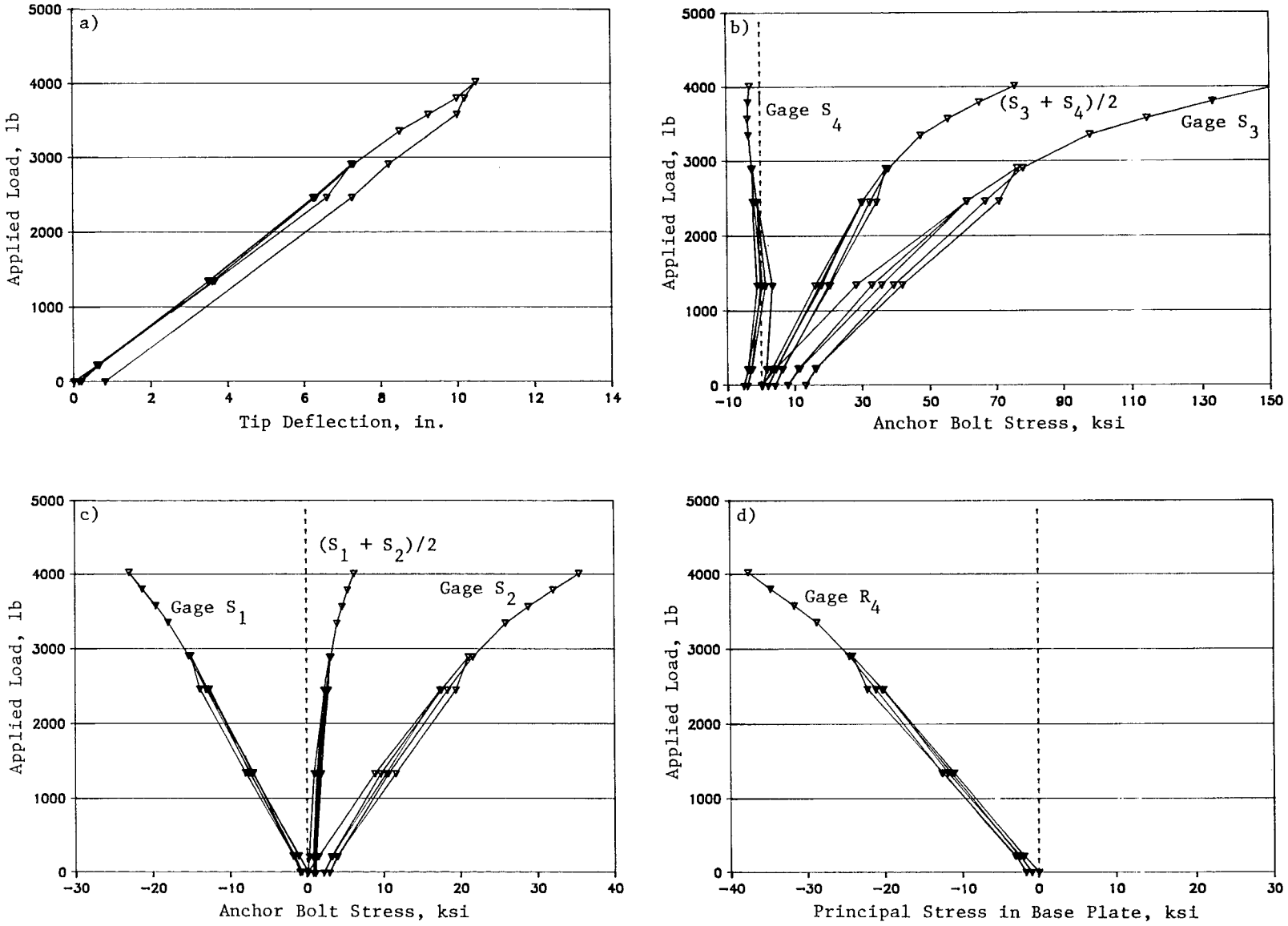

extrapolation leads to a stress of 42.9 ksi at the 5,000-lb design load, which is 29 percent higher than 33.3 ksi (0.924 F_y), indicating the base plate's inadequacy. Comparison of Figures 9d and 11d (for Poles C530(T) and C530) indicates that the thinner base plate experienced much higher stresses under the same load levels. This clearly demonstrates the contribution of base plate thickness to the pole's strength.

f. Load Test 5

Pole C832 was loaded diagonally, with strain gages on the post under tension (Table 2 and Fig. 7). The pole was loaded up to 5814 and 7155-lb in two successive cycles; Figure 12a shows the load-deflection curve from this test. Residual displacements were observed at the ends of both cycles. Yielding began at a load between 4696 and 5814 lb. The anchor bolt in compression (Gage S13 in Fig. 12b) experienced very high stress under loads within this range, exceeding its actual and nominal yield stresses (58.8 and 50 ksi). Stress due to axial force, obtained by averaging the two strain-gage readings (S12 and S13), was -36.0 ksi under 4696 lb of the first loading cycle, where yielding had not yet begun. By linear extrapolation, this stress would become 61.3 ksi under the design load of 8000 lb. This level is significantly higher than the nominal yield stress (F_y = 55 ksi). The anchor bolts thus were inadequate.

Under the base plate strain gages, R8 and R10 showed highest stress levels. For example, maximum prinicipal stress at R8 due to a 4696-lb load was 21.2 ksi in compression. It would reach 33.3 ksi (0.924 F_y) at 7376 lb (8 percent lower than the 8000-lb design load) by linear extrapolation. Since R8 was not necessarily at the most critical section of the base plate, it was concluded that this plate was structurally inadequate.

g. Load Test 6

Pole C832 was reset in this test for parallel loading as shown in Figure 7 (see also Table 2), and loaded through five cycles. Figure 13a shows the load-deflection curve, and Figure 13b shows that the anchor bolt (S10 in Figure 13b) again was the first component to yield. Significant yielding occurred at a load between 5814 and 7155 lb. It is interesting to note that as expected, axial stress in this test was much lower than in Test 5 (under diagonal load), indicating adequacy of anchor-bolt axial strength under the parallel load. This clearly shows that the diagonal load is the governing loading case for the anchor bolts, a fact apparently neglected in designing these poles.

Of all the base plate strain gages, R10 and R8 showed the highest stress levels under loading. For example, maximum principal stress at R10 due to a 3578-lb load was 21.5 ksi in compression. It would reach 33.3 ksi (0.924 F_y) at 5542 lb by linear extrapolation. This is much lower than the pole's design capacity of 8000 lb, and clearly demonstrates the base plate's deficiency.

Figure 12. Load Test 5: Pole C832 under diagonal load.

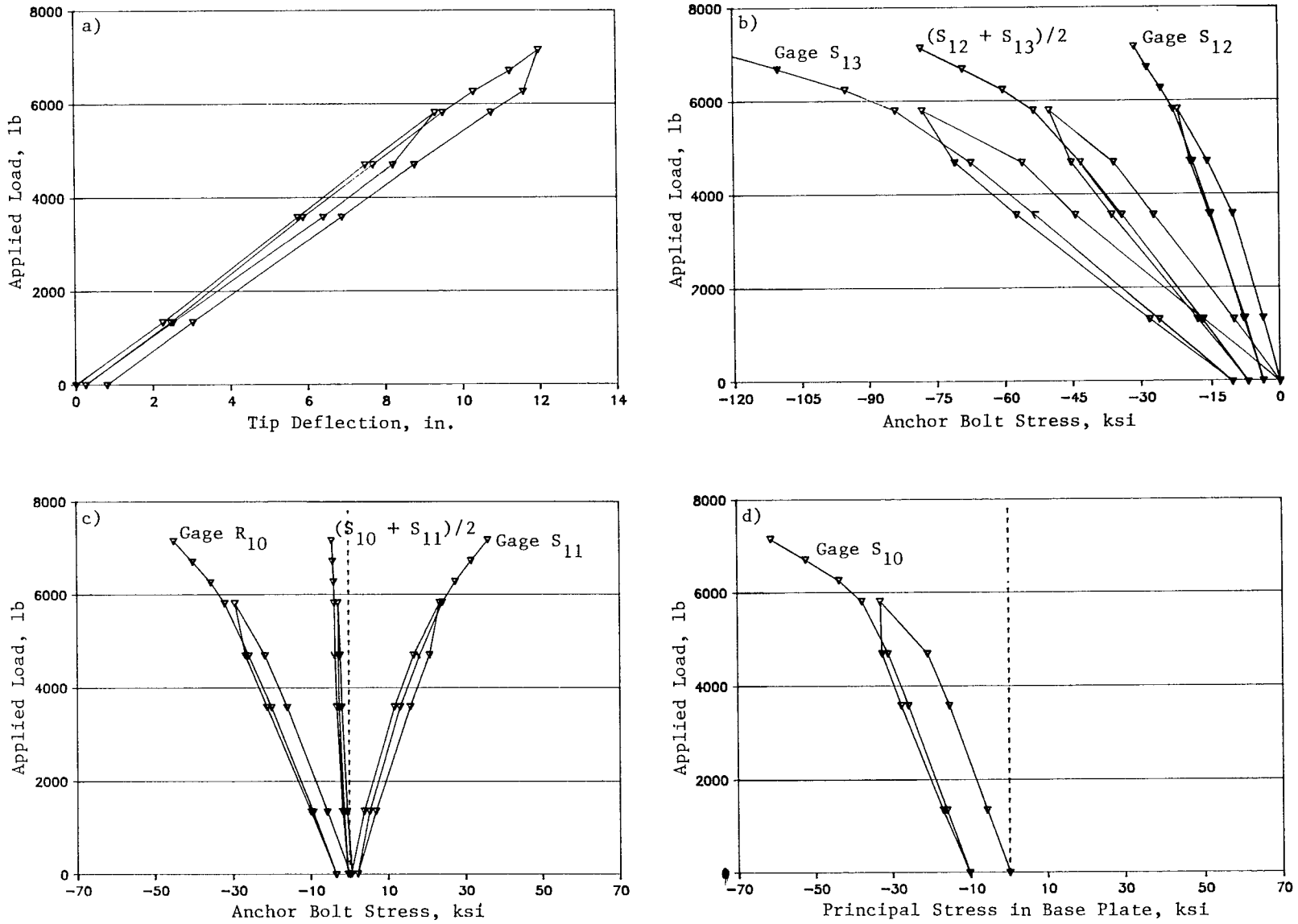

Figure 13. Load Test 6: Pole C832 under parallel load.

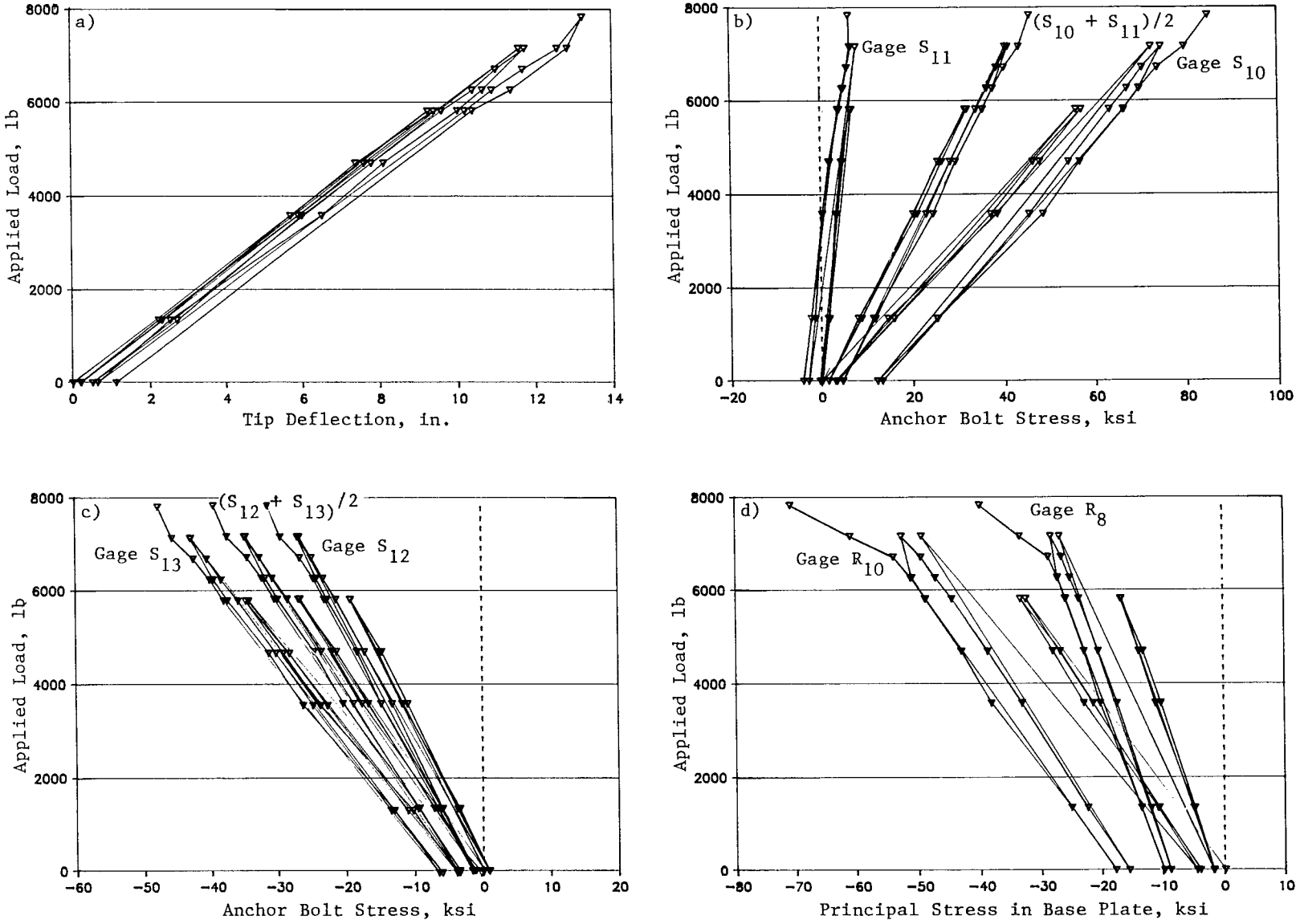

D. Summary

Based on results of the material tests and full-scale load tests, the following conclusions are drawn:

1. Except for the C832 base plate and post, material strengths of the posts, base plates, and anchor bolts exceeded their nominal values. The base plate for Pole C832 had a yield strength of 29.0 ksi, lower than its 36-ksi nominal value. Its post had a yield strength of 47.3 ksi, lower than its 50-ksi nominal value.

2. The three standard poles tested (C326, C530, and C832) were structurally inadequate. The deficient components were the base plate and anchor bolts. It is noted that the deficiency in anchor bolts is apparently due to failure to recognize diagonal load as the critical loading case. On the other hand, yielding of the anchor bolts in load tests was initiated mainly because of 1) significant bending caused by the unfilled space between the base plate and foundation (Fig. 4), and 2) uneven reduction of their tensile and bending capacities caused by grinding-off metal for strain gage installation.

III. FINITE ELEMENT ANALYSIS (FEA)

FEA was used to analyze the signal poles, due to lack of a closed-form solution for the problem. The computer analysis was performed using Graphics Interactive Finite Element Total Systems Software (GIFTS) (3). Analysis was limited to the linear elastic range due to the software's capability.

A. Modeling Details

To minimize the number of elements used and thereby reduce computing time and modeling effort, two quarter-models were generated to analyze the poles under separate diagonal and parallel loadings. The quarter-models take into account symmetric and antisymmetric behaviors of the structure under the applied loads. Figure 14 shows the FEA quarter-models for the parallel and diagonal loadings. Figure 15 shows element meshes for these two models, whose details are discussed here.

1. Modeling of the Post

Solid elements (SLD8 in Ref. 3) were used to model the post's lower 15 in., where a finer mesh of elements was necessary to examine stress concentration near the post's base. Plate elements (QB4 in Ref. 3) were then used to model the rest of the post. This combination of elements was selected to reach an acceptable accuracy in results and an affordable number of elements.

2. Modeling of the Hand Hole

A separate model was developed to examine stress distribution at the hand hole and adjacent reinforcement. The entire post was modeled using plate elements (QB4 in Ref. 3). The post was modeled as a cantilever beam fixed at its base. Analysis was performed for the hand hole located perpendicular and parallel to the direction of the span wire.

3. Modeling of the Base Plate

Due to the relatively high ratio of thickness T to side length L in the base plates, solid elements (SLD8) were considered more appropriate than plate elements (QB4) for modeling of the base plate. Five layers of solid elements were used through the depth of the plate. The layers were 0.2 to 0.75 in. thick with the surface layers thinner than the others. This allowed the

Figure 14. Quarter models and their boundary conditions.

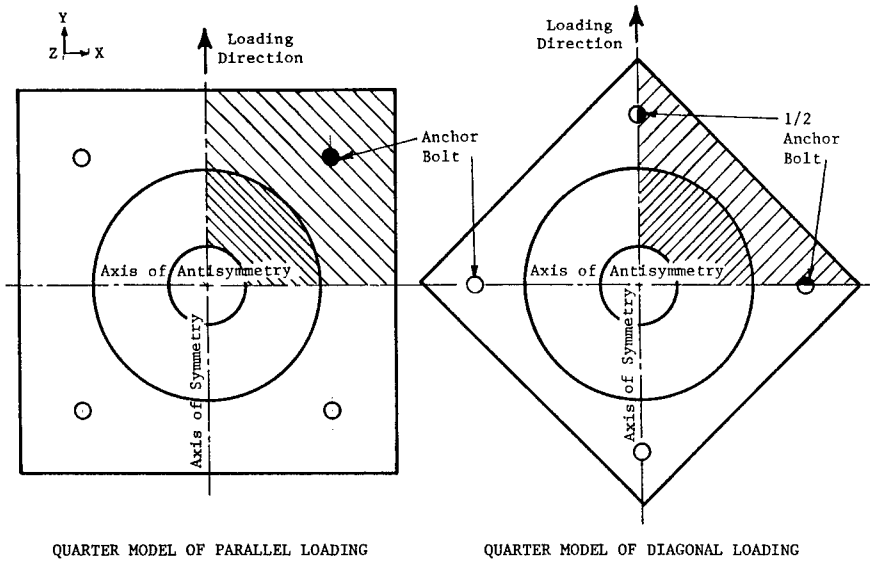

Figure 15. Typical FEA quarter models.

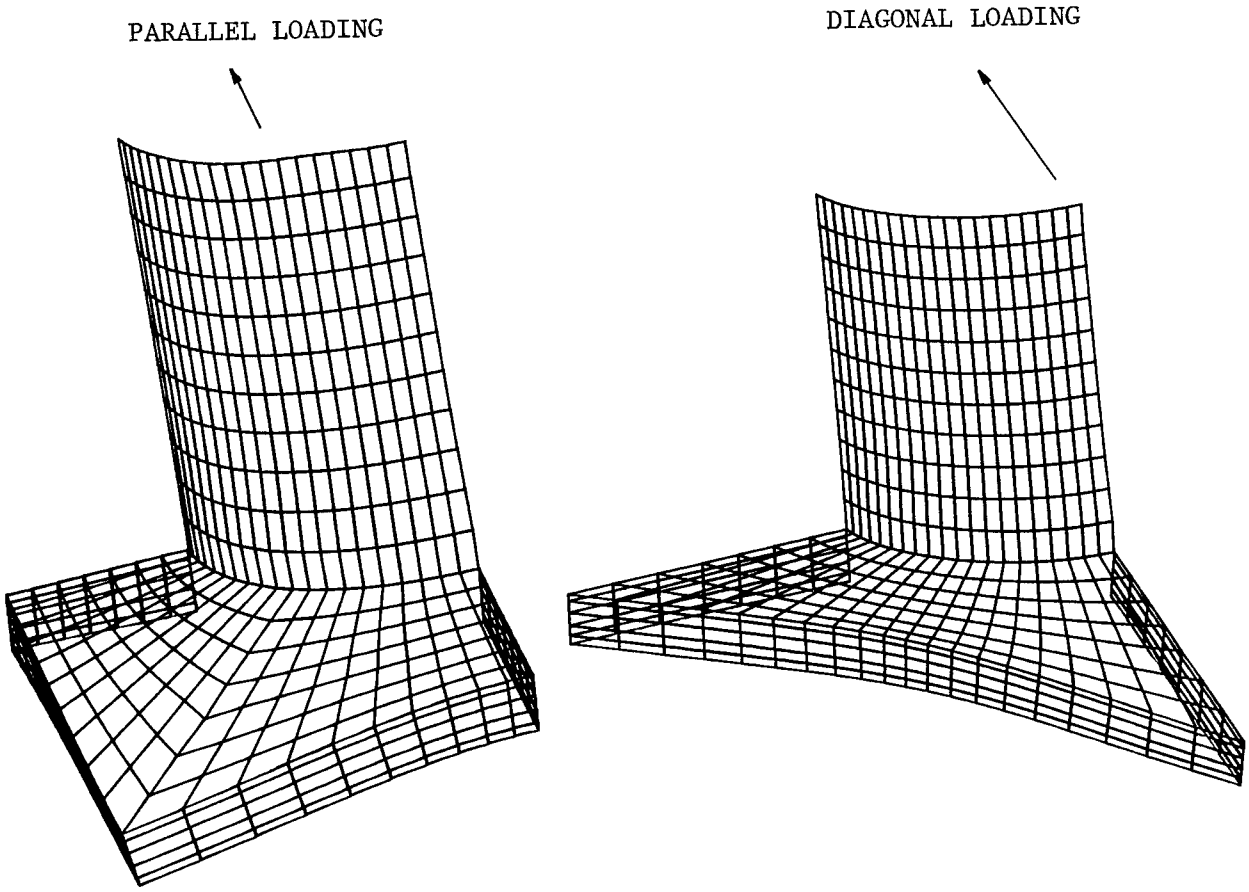

center of the top layer, where stresses were calculated, to be close enough to the top surface of the base plate, where strain/stress readings were obtained in the load tests, for practically realistic comparisons. Accordingly, FEA stress results could be directly verified by test results without significant loss of accuracy.

4. Modeling of the Anchor Bolt

Beam elements (BEAM2 in 3) were used to model the anchor bolts. Each bolt was connected at one end to a node at the top surface of the base plate and assumed fixed at the other end (foundation). For the diagonal loading case, where the anchors are on the axes of symmetry and antisymmetry (Fig. 14), only half of the anchor bolt cross-section areas were used in modeling to account for this. Concrete packing was not included in modeling to simulate a critical service condition represented in the load tests.

B. Validity of FEA Modeling

Results of the load test and FEA of Posts C326, C530, and C832 are discussed in this section, to examine validity of the FEA modeling. The physical quantities considered are tip deflection, anchor force, and stresses in the base plate and post. FEA analysis results for the hand hole are also included here. Due to GIFTS' capability for only linear analysis, comparison between the test and FEA results is limited to the linear elastic range before yielding.

1. Tip Deflection

Figure 16 shows comparison of tip deflection results by FEA and the tests for Poles C326 (Load Test 1), C530 (Load Tests 3 and 4), and C832 (Load Tests 5 and 6), within the elastic range. It is seen that FEA has predicted the tip deflections in good agreement with those by the load tests, especially when the loads were relatively low, i.e., when the poles were still in the elastic range. Note that Pole C530(T) (Load Test 2) is not included because it was not a standard pole.

2. Bending Stresses in the Post Near the Base

Test results indicated that the posts were structurally adequate. Bending stresses recorded from the single-arm strain gages agreed well with FEA results, and also with design calculations based on beam theory, assuming the pole to be fixed at its base (a cantilever beam). For example, Gage S7 on Pole C530 in Load Test 4 (see Fig. 6 for location) showed 20.6 ksi bending stress due to a 2460-lb diagonal load, and FEA and beam theory results were 22.1 ksi and 21.5 ksi, respectively. Gage S14 on Pole C832 in Load Test 5 (see Fig. 7 for location) showed a bending stress of 22.4 ksi due to 4696 lb of diagonal load. Similarly, Gage S15 in Load Test 6 (see Fig. 7 for location) showed a bending stress of 20.9 ksi due to 4696 lb of parallel load. For comparison, the corresponding FEA and beam theory results were 22.3 and 23.1 ksi, respectively.

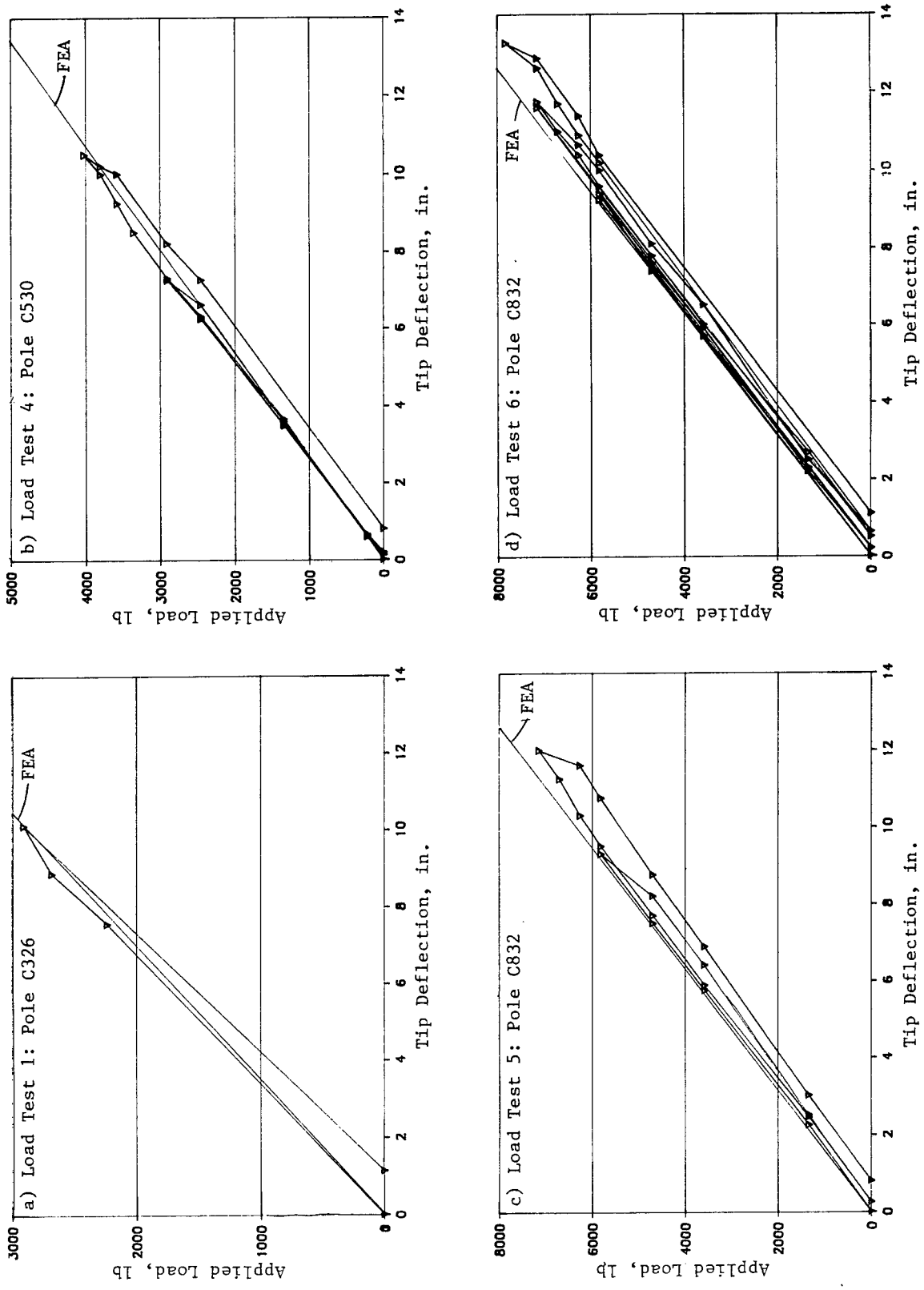

Figure 16. Tip deflection comparison.

Table 4. Numerical comparison of testing and FEA results for base plate stress (Pole C832) under diagonal 3578-lb load).

Strain Gage ID	Stress Components, ksi						Dominant Stress Component	Difference, %
	Test			FEA				
	Sx	Sy	Txy	Sx	Sy	Txy		
R7	+0.53	-0.53	+4.02	+0.27	-1.35	+4.73	Txy	+17.7
R8	+0.26	-13.20	+6.00	+0.32	-13.19	+6.26	Sy	+0.1
R9	-1.98	-5.00	-7.85	-2.24	-7.78	-8.20	Txy	+4.5
R10	+0.23	-13.22	-6.00	+0.32	-13.19	-6.26	Sy	+0.2

3. Stresses in the Base Plate

Figure 17 permits comparison of test results and FEA for the base plate in Load Test 4. Only the dominant component S_y (bending stress in y direction defined in Fig. 6) of Gage R4 showing the maximum response is plotted. Similar comparisons are shown in Figures 18 and 19 for Load Tests 5 and 6, respectively. The reader is referred to Figures 6 and 7 for stress coordinate systems of these cases. Figures 17, 18, and 19 show that FEA has accurately predicted base plate response within the elastic range. These areas also experienced the largest deflections according to FEA and test data, although base plate deflections were not recorded in the testing. These results also confirm the deficiency of base plates of the tested poles.

Table 4 provides numerical comparison of testing and FEA results for Pole C832 (Load Test 5) as a typical case of including nondominant components of stress. These are consistent with one another, especially for the pronounced stresses indicating critical response to load. Relatively larger differences (for example, in R7) are attributed either to inevitable discrepancy between locations of a strain gage and its corresponding element, or to higher noise-to-signal ratio in test data acquisition when the strain/stress signal was low.

4. Stresses Around the Hand Hole

Figure 20 shows FEA results for stress distribution at the hand hole of Pole C832 as a typical case. Load Cases I and II for the hand hole are respectively perpendicular and parallel to the span wire. Note that Case II is more critical for the hand hole. These results agree with those of the current design method, which checks bending stress of a beam with an open cross-section.

5. Stresses in the Anchor Bolts

Test results indicated that anchor bolts not located at the neutral axis were exposed to significant bending under loading, in addition to axial force. This anchor bending was noticed for both parallel and diagonal loadings. As expected, diagonal loading is more critical for anchor bolts, since only two

Figure 17. Base plate stress comparison: Load Test 4, Pole C530 (Bending).

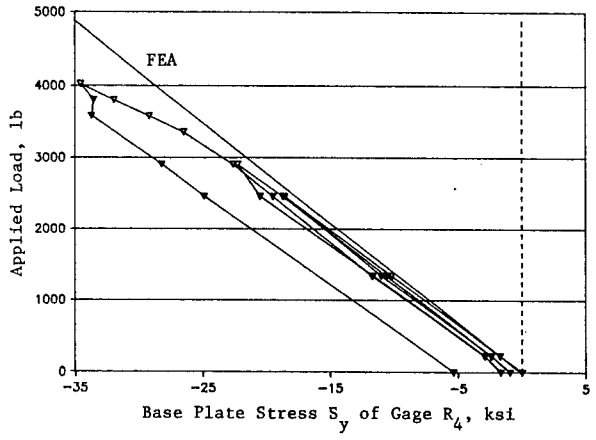

Figure 18. Base plate stress comparison: Load Test 5, Pole C832.

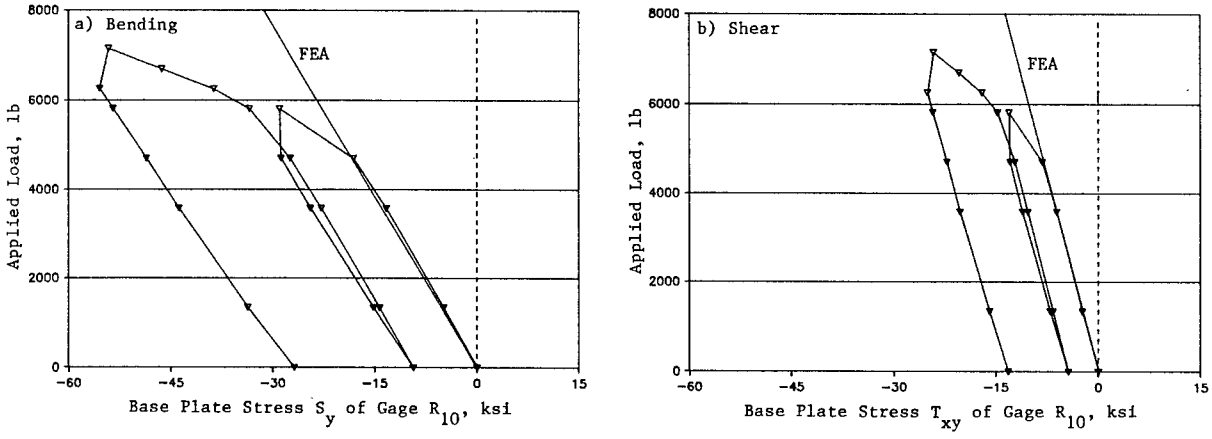

Figure 19. Base plate stress comparison: Load Test 6: Pole C832.

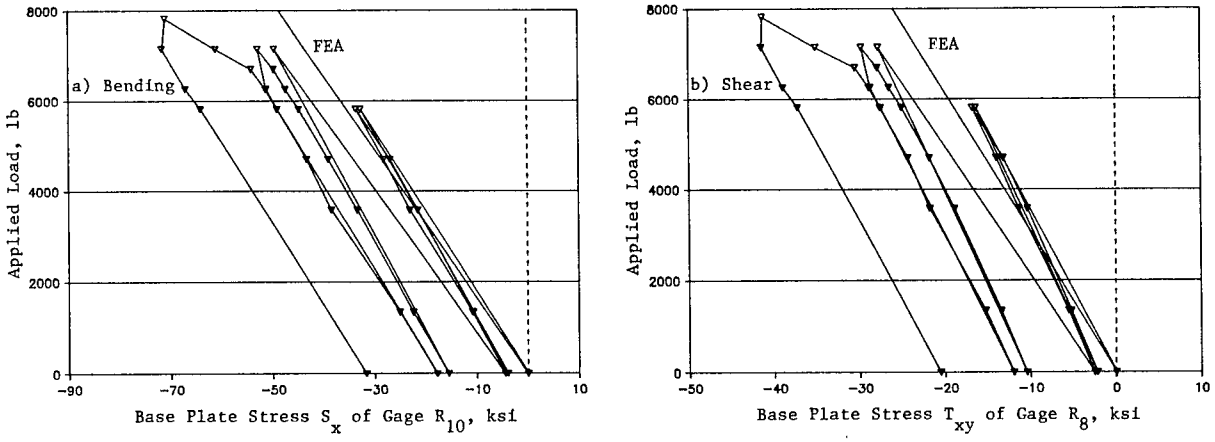

Figure 20. FEA results for Pole C832 hand hole: maximum principal stress contours in ksi (- for compression, + for tension).

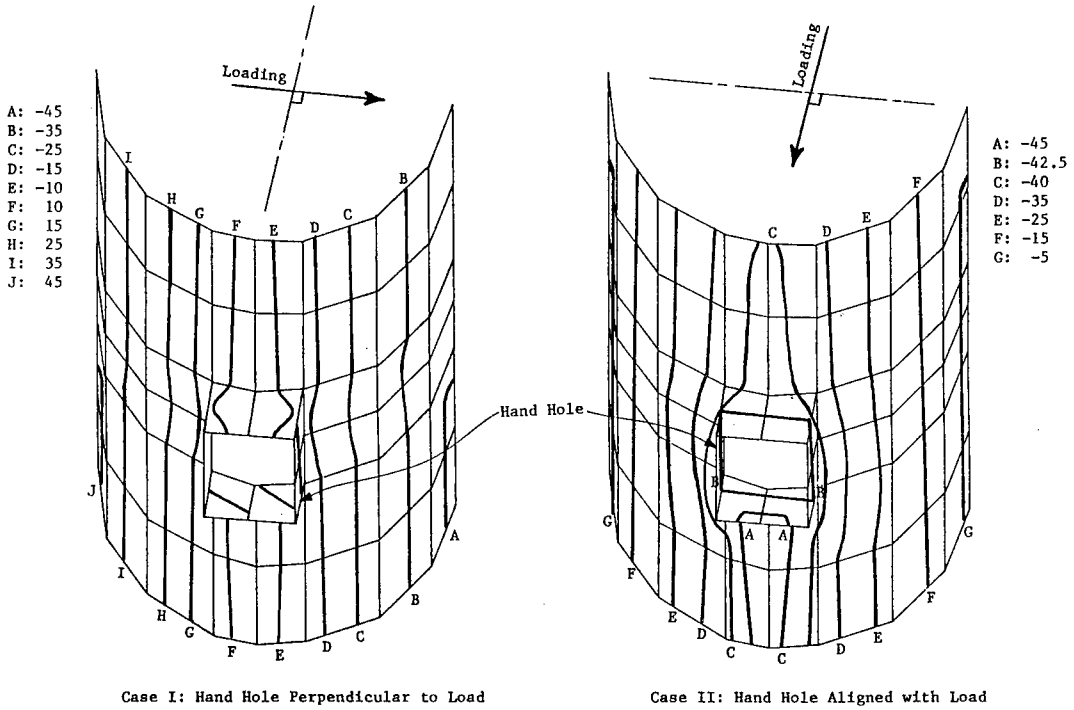

Figure 21. Anchor bolt stress comparison: Load Test 4, Pole C530.

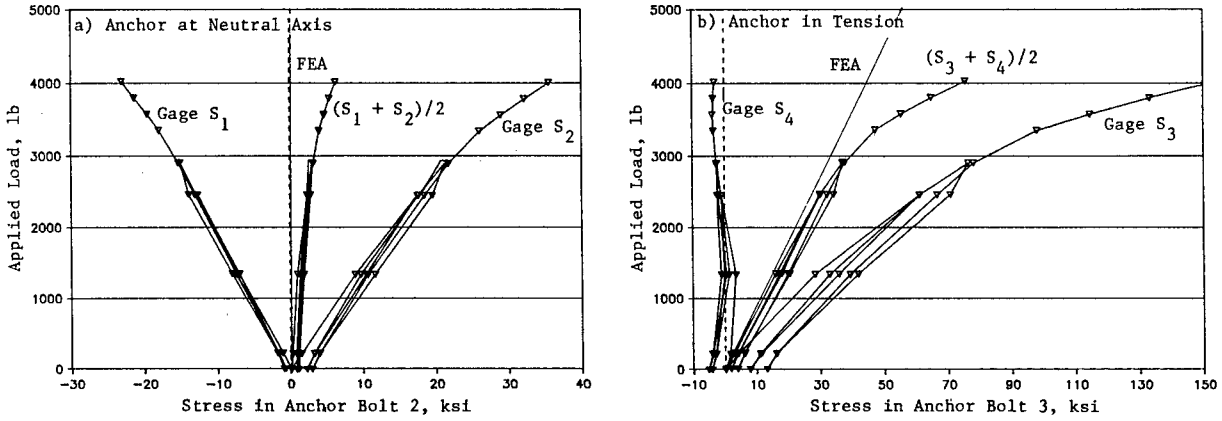

Figure 22. Anchor bolt stress comparison: Load Test 5, Pole C832.

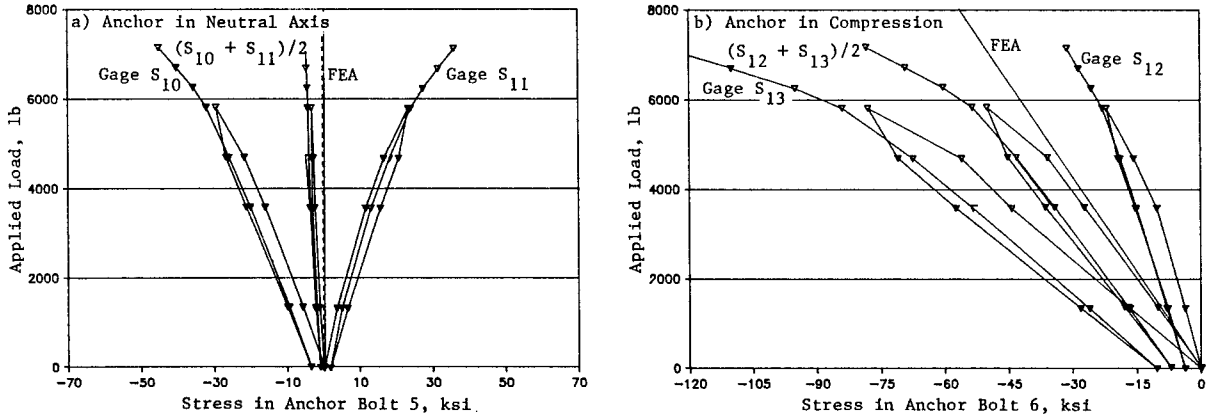

Figure 23. Anchor bolt stress comparison: Load Test 6, Pole C832.

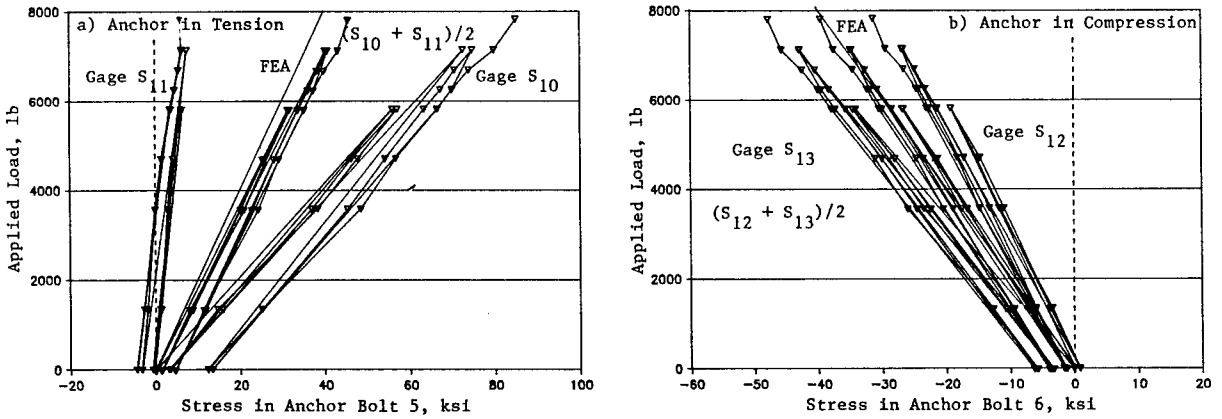

anchors are resisting the applied load. FEA results agreed well with test results with respect to axial force, as shown in Figures 21, 22, and 23 for Load Tests 4, 5, and 6, respectively. A reduced cross-section area (Fig. 24) is assumed equal to 0.75 times the gross area, which is a 5-percent reduction from the effective area calculated according to the current code (2). These figures demonstrate the efficiency in the anchor bolts.

C. Structural Adequacy of Existing Signal Poles

1. General Behavior of the Base Plate

Structural adequacy of a number of existing poles was evaluated using the FEA models just described. Base plates and anchor bolts were examined in this evaluation, since their deficiency had been established by the full-scale testing and FEA. General behavior of the base plate under the two critical loading cases (diagonal and parallel) is outlined in this section. Critical areas are identified here for attention in evaluation, as well as design.

Figure 25 shows a typical case of stress contours (on the top surface) and deflection distribution of a base plate under diagonal loading, obtained by FEA. Stress is expressed by percentage of overstress using the Von Mises criterion against nominal stress F_y = 36 ksi. Figure 25 shows a shaded area to indicate a critical region (120 and 130 percent of 36 ksi), which is obviously associated with the deflection shown. Figure 26a shows a typical case under parallel loading. Stress is again expressed by overstress percentage, the same criterion as in Figure 25. Figure 26a shows two shaded areas as critical regions in this case. Note that they represent maximum stress under the given load contributed by the dominant bending component (S_x in Region B) and shear component (T_{xy} in Region C). Figure 26a also shows displacement distribution associated with the stress field, compared with an actual deflection distribution in Figure 26b for a case of pole failure under parallel loading. This accident occurred when a truck caught the span wire and bent two poles over. The three critical regions (A, B, C) indicated in Figures 25 and 26 are thus considered in evaluating existing poles and developing a new design method.

2. Results of Evaluation for the Existing Poles

The verified FEA quarter-models were used to evaluate a representative sample of poles manufactured by New York State's three major pole suppliers: Carlan Manufacturing Co., Summit Manufacturing Inc., and Union Metal Corporation. This sample is listed in Table 5 with dimension details.

Each pole was analyzed under parallel and diagonal loads. Maximum principal stress (under diagonal load) and bending and shear stresses (under parallel load) in the base plate are recorded in Table 6. These were checked against factored allowable design stress specified in the current code (2). The extent of deficiency, if applicable, was accordingly determined by the percentage of overstress. Similarly, axial stresses in the anchor bolts are

Figure 24. Anchor bolt section loss for strain gage instrumentation and its effect.

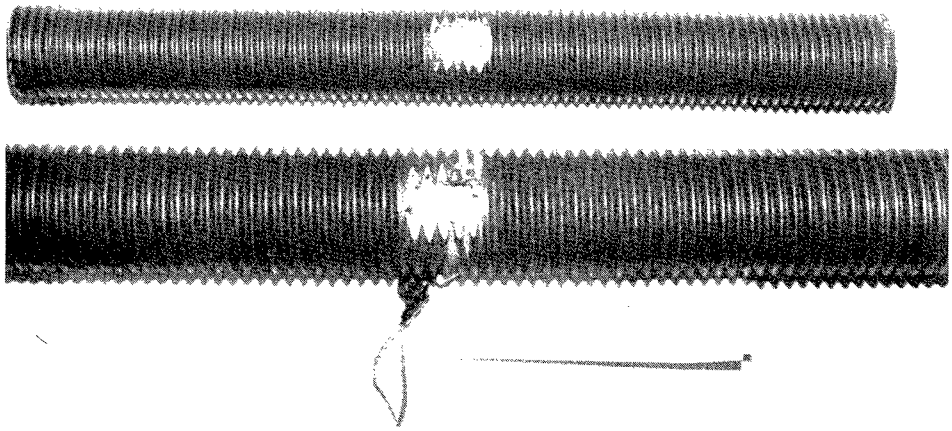

Anchor Bolt Section Loss

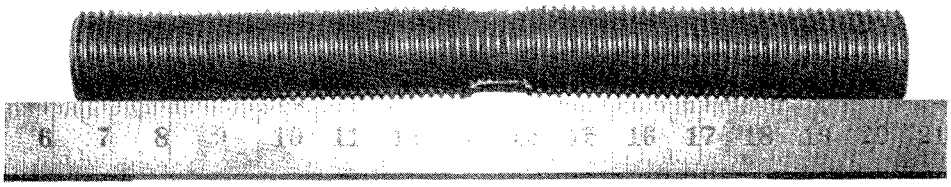

Residual Deflection at Reduced Section

Figure 25. Typical deflection and stress distribution under diagonal load (Pole C530, 5 kips).

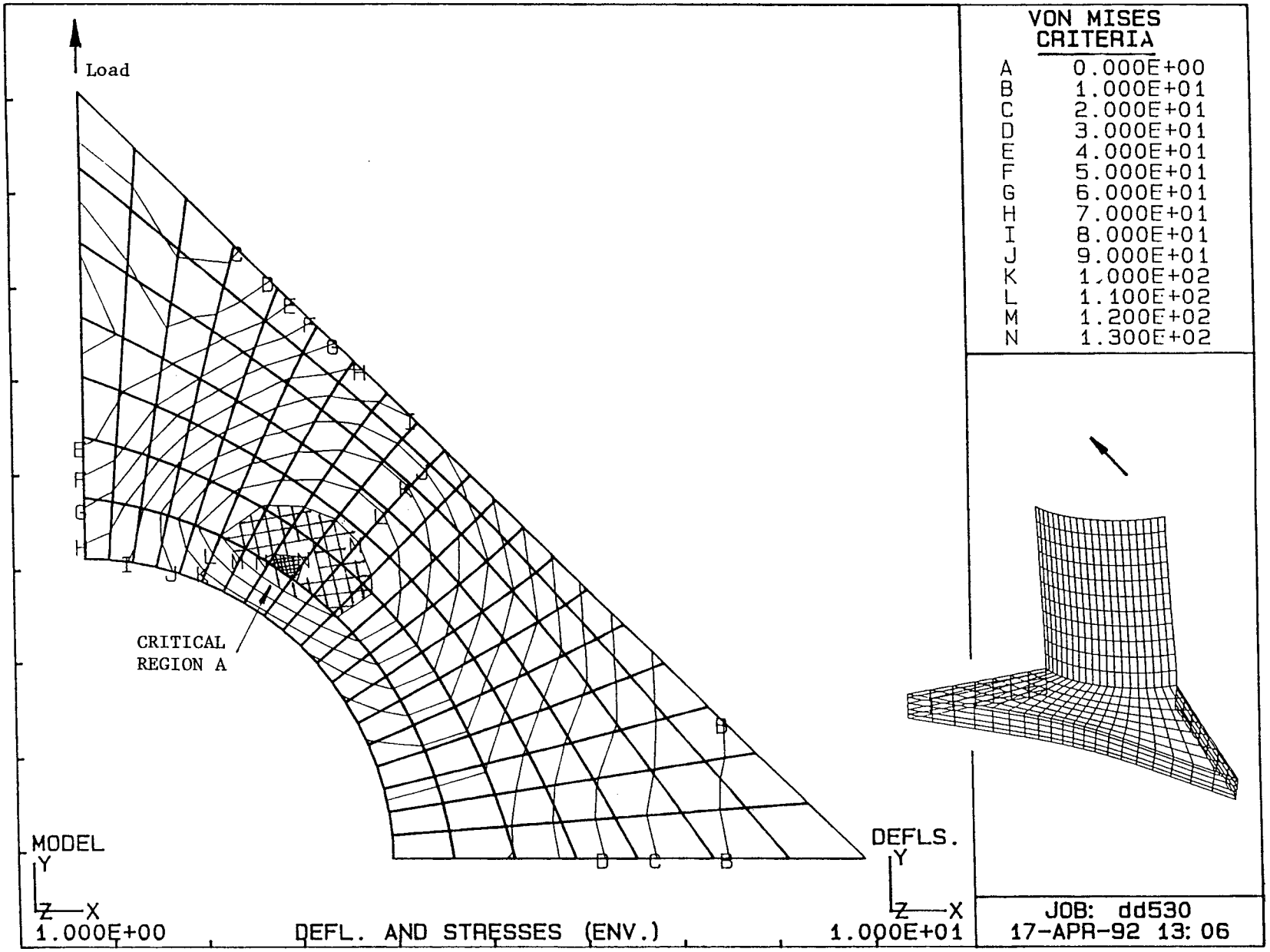

Figure 26a. Typical deflection and stress distribution under parallel load (Pole C520, 5 kips).

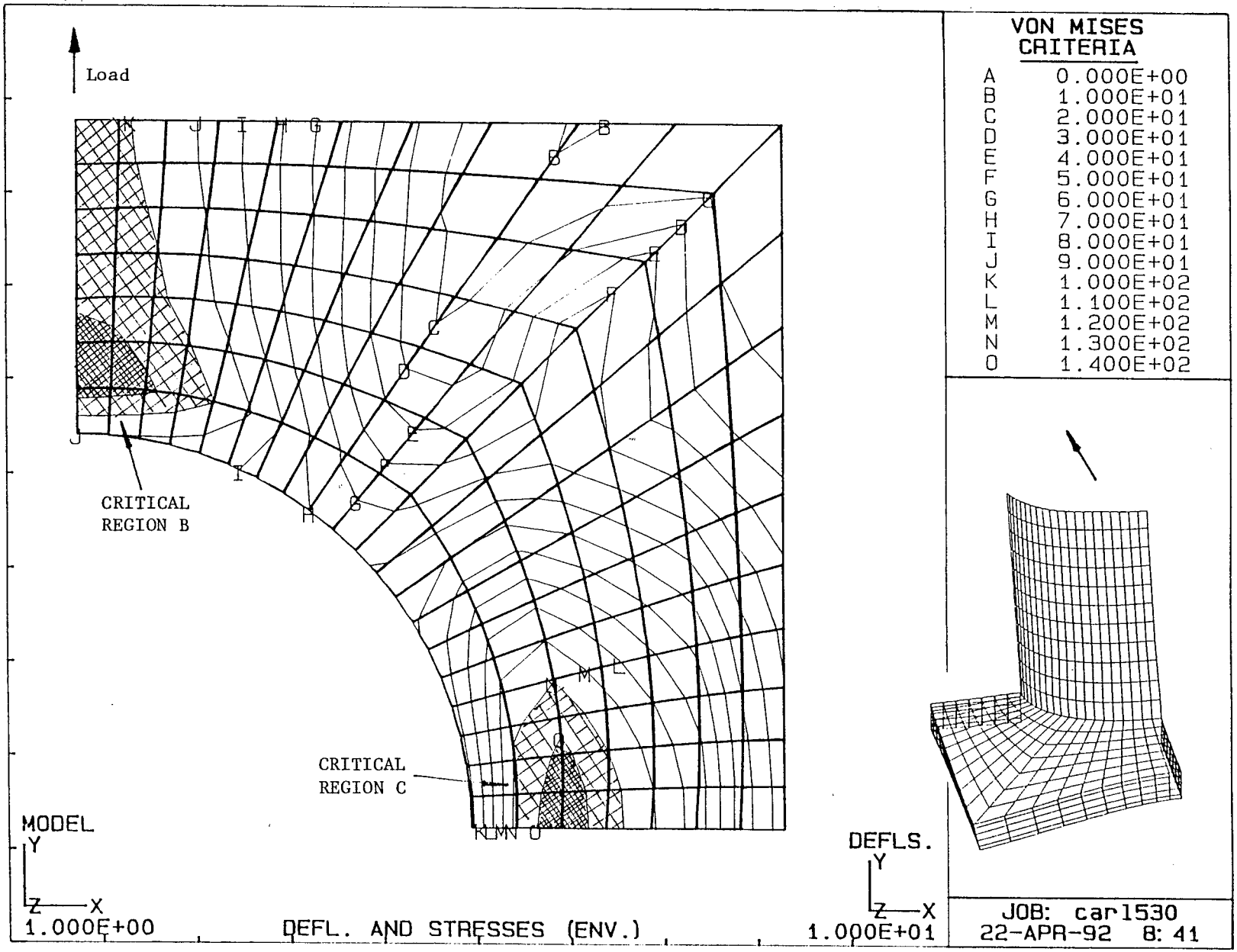

Figure 26b. Actual residual deflection due to parallel loading in an accident.

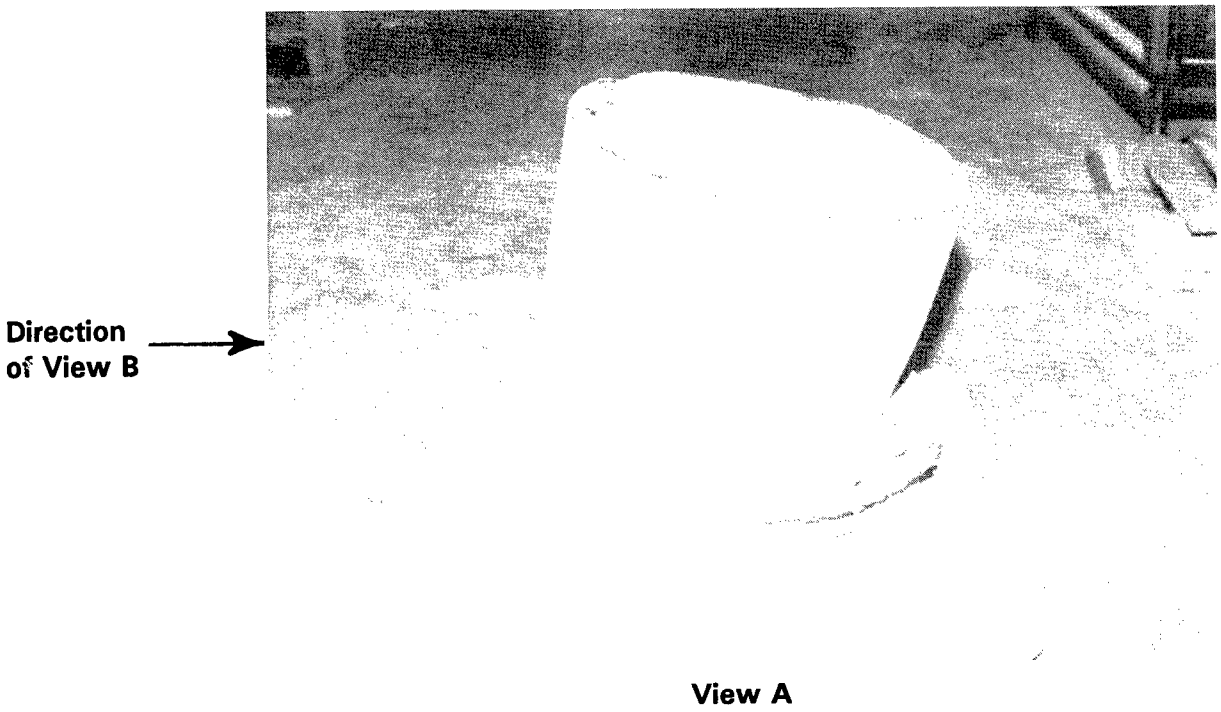

View A

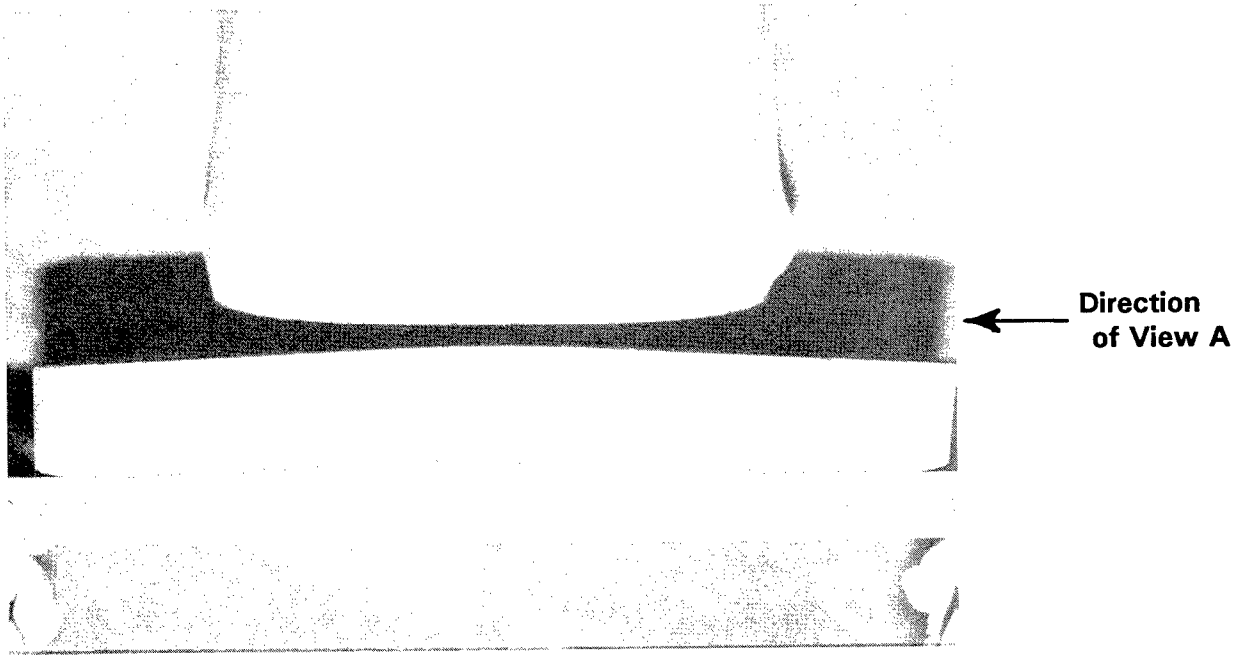

View B

Table 5. Dimension details of sample poles.

Pole ID	Post Dimensions, in. DT	DB	W	Base Plate Dimensions, in. L	T	BC	Anchor Bolt Dimension AD, in.
A. CARLAN POLES (Carlan Mfg. Co.)							
C326	8.625	10.75	0.250	17.0	1.50	17.0	1.25
C328	8.625	10.75	0.250	18.0	1.50	18.0	1.25
C430	10.750	12.75	0.280	18.0	1.75	18.0	1.50
C530	10.750	12.75	0.313	23.0	1.75	23.0	1.50
C530'	10.750	12.75	0.313	18.0	2.00	18.0	1.75
C732	12.750	16.00	0.313	25.0	2.50	25.0	1.50
C832	12.750	16.00	0.375	22.0	2.25	22.0	2.00
B. SUMMIT POLES (Summit Mfg. Inc.)							
S324	7.00	10.00	0.188	21.0	1.50	21.0	1.50
S328	7.50	11.00	0.188	21.0	1.50	21.0	1.50
S334	8.50	13.00	0.188	27.0	1.50	25.0	1.50
S434	9.50	14.00	0.188	27.0	1.75	25.0	1.75
S530	10.50	14.50	0.188	27.0	1.75	25.0	1.75
S632	12.00	16.50	0.188	27.0	2.00	29.0	2.00
S832	15.00	19.00	0.188	32.0	2.25	32.0	2.00
S934	16.50	21.00	0.188	33.0	2.25	33.5	2.25
S1036	17.50	22.50	0.188	35.0	2.25	33.5	2.25
C. UNION METAL POLES (Union Metal Corp.)							
U226	6.86	10.50	0.179	14.1	1.50	14.0	1.25
U530	9.80	14.00	0.250	20.5	2.00	20.0	1.75
U636	11.68	16.72	0.250	26.0	2.00	23.5	1.75
U832	12.00	16.50	0.313	24.5	2.50	23.5	2.00
U840	11.00	18.50	0.313	26.0	2.50	25.0	2.25
U1040	15.40	21.00	0.313	27.5	2.75	27.5	2.25
U1044	15.80	21.50	0.313	29.0	2.75	28.0	2.25

*Dimension definitions (see Fig. 1):
DT = diameter at top of post
DB = diameter at bottom of post
W = wall thickness of post at its base
L = side length of square base plate
T = thickness of base plate
BC = bolt circle diameter
AD = anchor bolt diameter.

also given in Table 6. Note that the shear stress in the anchor bolts is included in this evaluation, because it is usually not dominant compared with axial stress.

As shown in Table 6, the Carlan base plates were found deficient with respect to the three possible failure modes. Based on recommendations of the Structures Division during the course of this study, Summit Manufacturing revised its pole design by upgrading to larger and thicker base plates made of a higher-strength material. Table 6 gives results for these upgraded base plates. Three cases show more than 7-percent overstress, indicating their structural inadequacy. Note that Summit's new design appeared inadequate with respect to the shear failure mode and resulted in consistently deficient base-plate shear strength. The Union Metal base plates analyzed also proved deficient (Table 6). Table 6 also shows anchor bolt deficiency of the Carlan and Union poles.

Table 6. Evaluation of existing signal poles: maximum vs. allowable stress.

Pole ID	Base Plate: Parallel Load Bending, ksi	Base Plate: Parallel Load Shear, ksi	Base Plate: Diagonal Load Principal, ksi	Deficiency, %**	Anchor Bolts: Diagonal Load Axial, ksi***	Deficiency, %**
A. CARLAN POLES (Carlan Mfg. Co.)						
C326	42	26	43*	29	53	37
C328	45	28*	42	39	54	40
C430	42	26*	40	29	54	40
C530	46	30*	48	49	53	37
C530'	45	28*	40	39	49	28
C732	32	22*	32	9	73	88
C832	48*	25	48*	44	53	38
B. SUMMIT POLES (Summit Mfg. Inc.)						
S324	40	27*	39	adequate	27	adequate
S328	45	29*	42	4	32	adequate
S334	47*	28	39	2	33	adequate
S434	41	28*	43	adequate	32	adequate
S530	44	30*	43	7	36	adequate
S632	50	34*	49	21	30	adequate
S832	45	29*	42	4	36	adequate
S934	46	32*	51	14	33	adequate
S1036	49	33*	48	18	39	adequate
C. UNION METAL POLES (Union Metal Corp.)						
U226	38*	20	32	14	43	11
U530	40	25*	41	24	44	15
U636	48*	27	39	44	55	43
U832	39	24*	37	19	50	29
U840	40	26	44*	32	47	21
U1040	49	30*	44	49	53	37
U1044	45*	25	45*	35	57	49

* Governing load case

** All design loads on poles are Groups II or III. Accordingly, factored allowable design stresses are 140 percent of unit allowable stresses (2): $1.4(0.5F_y) = 0.7F_y$ for anchor axial strength (38.5 ksi), $1.4(0.66F_y) = 0.924F_y$ for bending strength (33.3 ksi for poles initialed with C and U, and 46.2 ksi for poles initialed with S), and $1.4(0.4F_y) = 0.56F_y$ for shear strength (20.2 ksi for poles initialed with C and U, and 28.0 ksi for poles initialed with S), respectively.

*** Bolt cross-section area is taken as 0.8 times the gross area of threaded bolt.

D. Summary

The FEA models for base plates and anchor bolts used in evaluating existing poles have been critically examined for their validity. Load tests and FEA identified critical areas for attention in evaluation, and highlighted three areas of stress concentration under two critical loading cases for base plates, and axial stress under diagonal load for anchor bolts. Stress levels in these areas were used for strength evaluation of existing poles from three major manufacturers for New York State. Anchor bolt and base plate designs of two vendors were found inadequate. The third upgraded his design, which was then found adequate for the anchor bolts. It also reduced the inadequacy of the base plates, but still failed to cover the shear failure mode.

IV. DESIGN METHOD FOR SIGNAL POLES

The current design method has been reviewed using data provided by full-scale testing and FEA. Conclusions and recommendations regarding this method are included here.

A. Post

The current design method based on the beam theory is adequate.

B. Hand Hole

The method (checking bending stress of a beam with an open cross-section) appears adequate. The critical orientation of load (wire) is normal to the plane of the hand hole (Case II in Fig. 20). It is recommended that the reinforcement be made of the same high-strength steel as the post, since some hand hole reinforcement was found inadequate. It is also recommended that the hand hole be located perpendicular to the span wire and along the neutral axis of the section when the pole is erected (as shown in Case I in Fig. 20). This is to reduce the probability of high stress in service.

C. Anchor Bolts

It is concluded that diagonal load is more critical than parallel load for anchor bolts, and thus must be used for anchor bolt design. Further, current practice considers only axial force in design of anchor bolts, and neglects the effect of anchor bending caused by the unpacked space between the base plate and foundation (Fig. 4). The design concept is appropriate only if this space is absent. This type of connection has been extensively studied, with findings summarized as guidelines (4). It is thus recommended that this space be eliminated by concrete packing as soon as feasible after erection.

D. Base Plate

Current methods used by pole manufacturers to design base plates are inadequate. Accordingly, a simple semi-empirical design method for the base plate is suggested here, followed by illustrative examples of its application.

1. Proposed Design Method

This method is intended to be consistent with the current working stress design concept adopted by the current AASHTO code (2) with respect to strength requirements. It essentially provides an analytical methodology to obtain maximum stresses within the elastic range. Resulting stresses are to be used to design the base plate in meeting strength requirements:

$$f_b \leq k\ F_b$$

and

$$f_v \leq k\ F_v \qquad (1)$$

where k is given by the current AASHTO code (2) -- for example, 1.4 for Group II load, F is allowable stress, f is computed stress, and subscripts b and v indicate bending and shear stresses, respectively. Three critical stresses, corresponding to the critical regions identified in Figures 25 and 26, must be considered for proportioning.

This method uses the concept of decomposed-components to simplify the analysis, separately addressing the three critical regions. For each possible failure mode (or critical region), part of the base plate including the critical region is isolated and modeled by an elementary component (e.g., a beam). A critical cross-section is then identified, as well as the corresponding load. The following analysis becomes straightforward, based on the simplified analytical model, with assistance of an empirically determined equivalent coefficient to modify the section's elastic capacity. These equivalent coefficients were determined empirically by considering twenty-three representative signal poles designed by three major New York State suppliers, and five of their modifications of selected deficient poles. Dimensions of these poles are given in Tables 5 and 7. Note that the modifications were done respectively based on S632, S934, U226, and U1040, and the resulting poles are identified accordingly without the initial letter for the manufacturer. Their steel strengths are assumed as indicated in Table 7, and were used as requirements in the process of redesign.

Bending Stress due to Diagonal Loading (for Critical Region A in Fig. 25)

f_b = Anchor Force x Moment Arm/Equivalent Flexural Elastic Section Modulus

$$= (M/BC)(BC - DB/2)/\alpha\{(1.414\ L - DB)\ T^2/6\} \qquad (2a)$$

Eq. 2a is obtained by simplifying the problem as a cantilever beam under a concentrated load at its free end, applied by an anchor bolt as shown in Figure 27. This assumes that the critical point being checked is on Section S_a as shown. M is moment at the post base due to the design load; BC, DB, L, and T have been defined in Table 5 and shown in Figure 1; M/BC is the axial anchor force; (BC-DB)/2 is its moment arm; $(1.414L-DB)T^2/6$ is the bending modulus of Section S_a; and α is an empirical coefficient:

Table 7. Modified base plate dimensions of selected sample poles.

Pole	Base Plate Dimensions, in. L	T	BC	Assumed F_y, ksi*
632	27.0	2.25	29.0	50
934(1)	33.0	2.75	33.5	36
934(2)	33.0	3.00	33.5	36
226	14.1	1.75	14.0	36
1040	27.5	3.25	27.5	36

*Assumed as requirement of redesign.

Figure 27. Simplified analysis model for maximum bending stress under diagonal load.

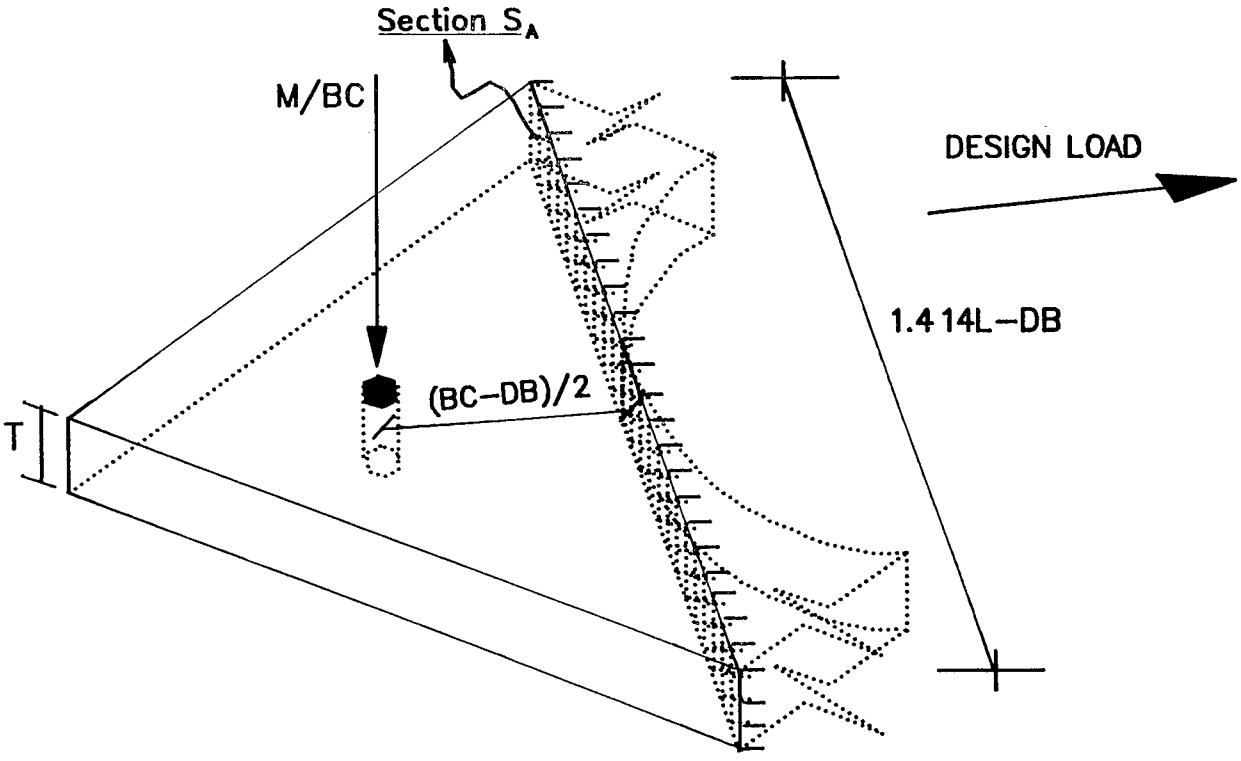

$$\alpha = \{4.304 - 0.02021BC/T - 4.304DB/L + 4.503(DB/L)^2 - \ldots$$
$$- 0.9750(L - 0.707BC)/(L - DB) - 1.686BC/L\}/C_\alpha \quad (2b)$$

$$C_\alpha = 1.097 \quad (2c)$$

Eq. 2b is obtained by a multivariable regression for the ratio of f_{FEA} (maximum stress by FEA) to f:

$$f = (M/BC)(BC - DB/2)/\{(1.414\ L - DB)T^2/6\} \quad (3)$$

α is thus considered an equivalent coefficient for the section modulus with respect to critical stress, as expressed in Eq. 2a.

Bending Stress due to Parallel Loading (for Critical Region B in Fig. 26a):

f_b = Midspan (Maximum) Moment/Equivalent Elastic Flexural Section Modulus

$$= 0.25M/(DB/L')^2\{1/4 - (1 - DB/L')/3 + (1 - DB/L')^4/12\}/\{\beta(L - \ldots$$
$$- DB)T^2/12\} \quad (4a)$$

This formula is derived by isolating a beam with both ends built-in and a span of 0.707BC under a triangularly distributed load applied by the post, as shown in Figure 28. Eq. 3a checks a critical point on Section S_b as shown. L' = max{0.707BC,DB} (max{ } means the maximum value of); $(L-DB)T^2/12$ is the bending modulus of Section S_b; β is an empirically determined coefficient:

$$\beta = \{157.6 - 21.85L/DB - 0.3300BC/T - 259.3DB/L - 48.13(L \times T/DB/$$
$$(L - DB))^{1/2} + 194.6\ (DB/L)^2 + 127.4T/BC - 21.65DB/BC\}/C_\beta \quad (4b)$$

$$C_\beta = 1.080 \quad (4c)$$

β is derived by the same method for α, with f_{FEA} for the corresponding case and

$$f = 0.25M/(DB/L')^2\ \{1/4 - (1 - DB/L')/3 + (1 - DB/L')^4/12\}/\{(L - \ldots$$
$$- DB)T^2/12\} \quad (5)$$

And β is an empirical coefficient for an equivalent cross-section modulus with respect to the critical stress, as formulated in Eq. 4a.

Shear Stress due to Parallel Loading (for Critical Region C in Fig. 26a):

f_v = Torque by Anchors/Equivalent Elastic Torsional Section Modulus

$$= (M/2)/\{\gamma\ C'\ b\ T^2\} \quad (6a)$$

Figure 28. Simplified model for maximum bending stress under parallel load.

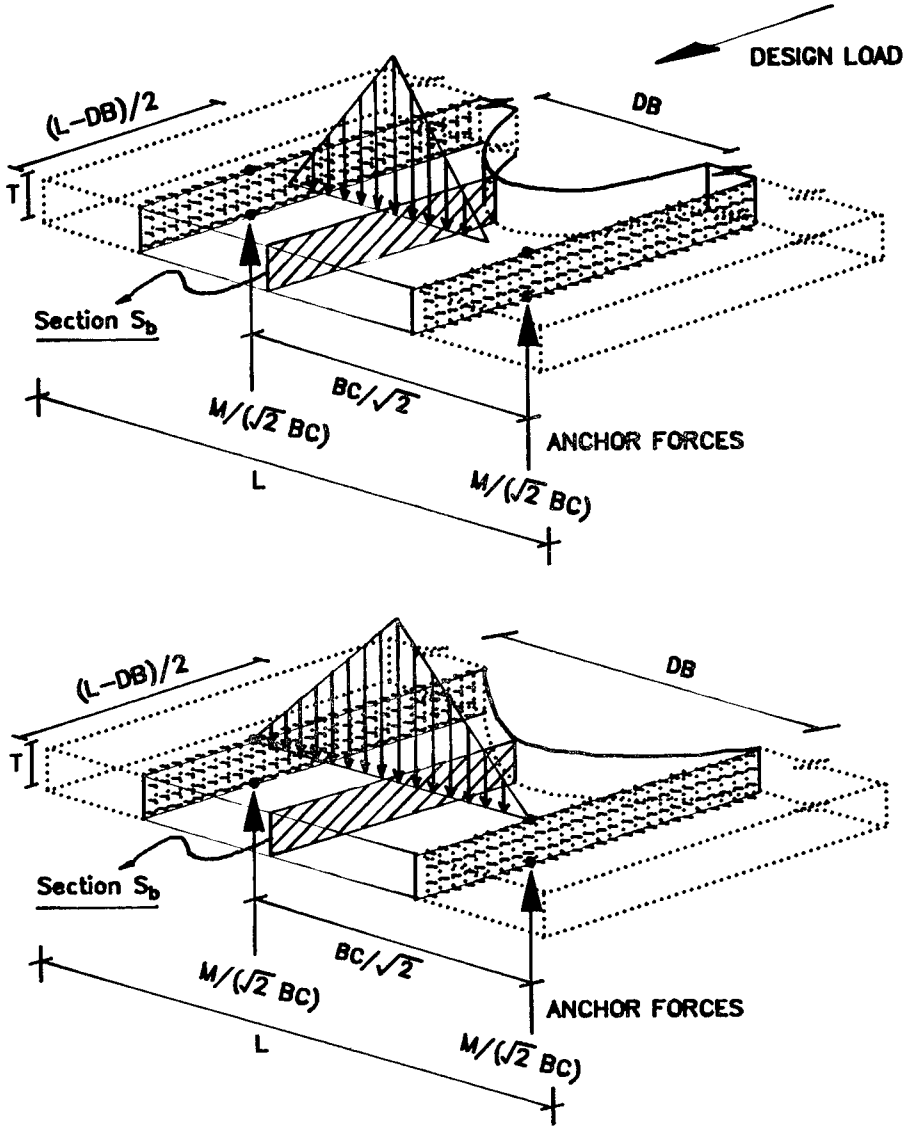

Eq. 6a is derived based on simplification of the problem by considering a rectangular bar under a torque (applied by a pair of anchor bolts), as shown in Figure 29. Maximum shear stress occurs on Section S_c. M/2 is the torque induced by the anchor forces, which in turn is due to the design load; b = min{0.707BC,DB} (min{ } means the minimum value of); $C'bT^2$ is the torsional modulus of Section S_c; C' is a coefficient given in Table 8 based on the elasticity solution, depending on ratio b/T (5); and γ is an empirical coefficient:

$$\gamma = \{210.0 - 66.9BC/DB - 0.1719(BC - DB)/T - 714.8DB/L + 358.3 (DB/L)^2 - 48.16(L-0.707BC)/(L-DB) - 288.2(BC-DB)/(1.414L-DB) + \ldots + 381.0BC/L\}/C_\gamma \quad (6b)$$

$$C_\gamma = 1.094 \quad (6c)$$

γ is found by the same method as α, with f_{FEA} for the corresponding case and

$$f = (M/2)/\{\gamma\ C'\ b\ T2\} \quad (7)$$

to modify the cross-section modulus for equivalence in critical stress, as expressed in Eq. 6a.

Figure 30 shows a comparison of computed stresses by the suggested method and F_{FEA} by FEA, for the three critical stress cases. The observed conservatism (overestimation) in computed stresses is introduced by an amplification factor $C_i = m_i + \sigma_i$ ($i = \alpha, \beta, \gamma$), where m_i ($m_i + \sigma_i$) and σ_i ($m_i + \sigma_i$) are respectively the mean and standard deviation of the ratio of stress by FEA to computed stress for respective critical stress cases. m_i and σ_i are found to be around 1.0 and 0.090 for each case, respectively.

2. Illustrative Examples

The suggested analytical method is applied here to Pole S632 for its evaluation and modification as an example for illustration. F_y = 50 ksi is used for proportioning, and $kF_b = 1.4 \times 0.66 \times 50 = 0.924 \times 50 = 46.2$ ksi and $kF_v = 1.4 \times 0.4 \times 50 = 0.56 \times 50 = 28$ ksi are assumed for Load Groups II and III.

Step 1: From Table 5, L = 27 in., T = 2.00 in., BC = 29 in., and DB = 16.50 in. By definition, the pole is 32 ft in height and its design load is 6 kips.

For maximum bending stress under diagonal loading

Anchor force = 6 x (32 - 1.5) x 12/29 = 75.72(kips).

Moment arm = 0.5 x (29 - 16.5) = 6.25(in).

Figure 29. Simplified model for maximum shear stress under parallel load.

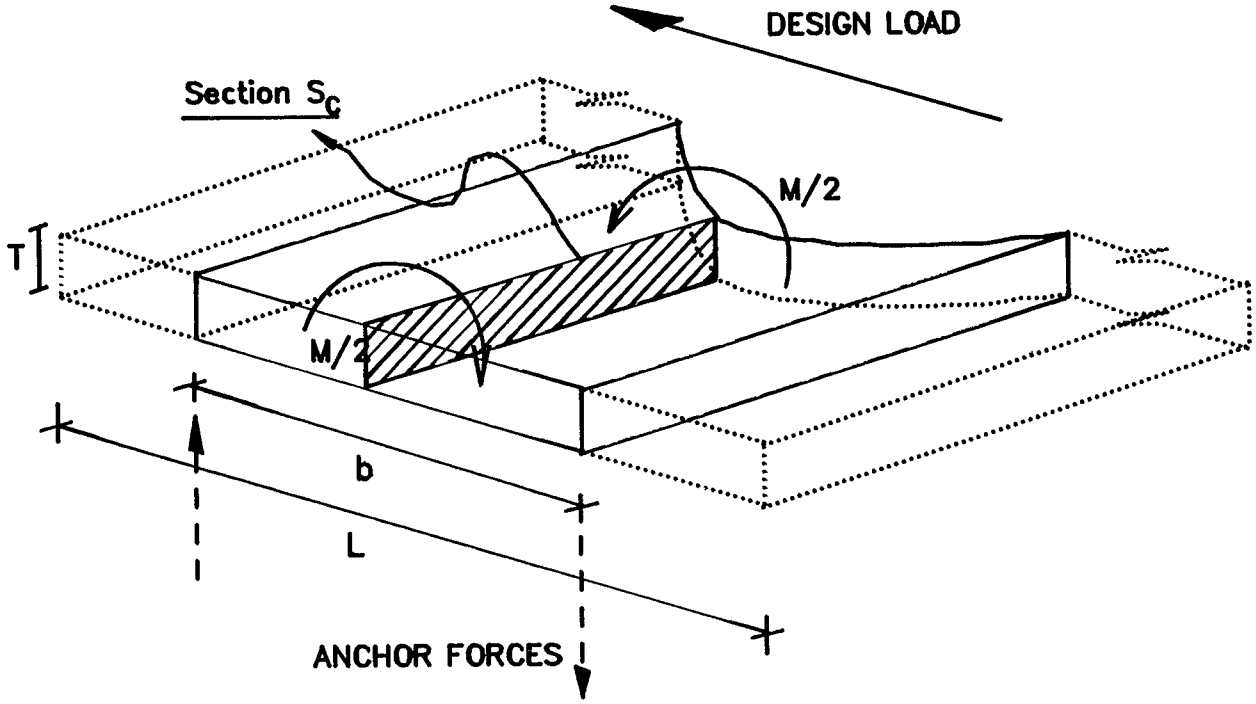

Table 8. Coefficient C' for torsion (5).

b/T	C'
1.0	0.208
1.2	0.219
1.5	0.231
2.0	0.246
2.5	0.258
3.0	0.267
4.0	0.282
5.0	0.291
10.0	0.312
∞	0.333

Figure 30. Comparison of critical stresses (ksi) by FEA and proposed design method.

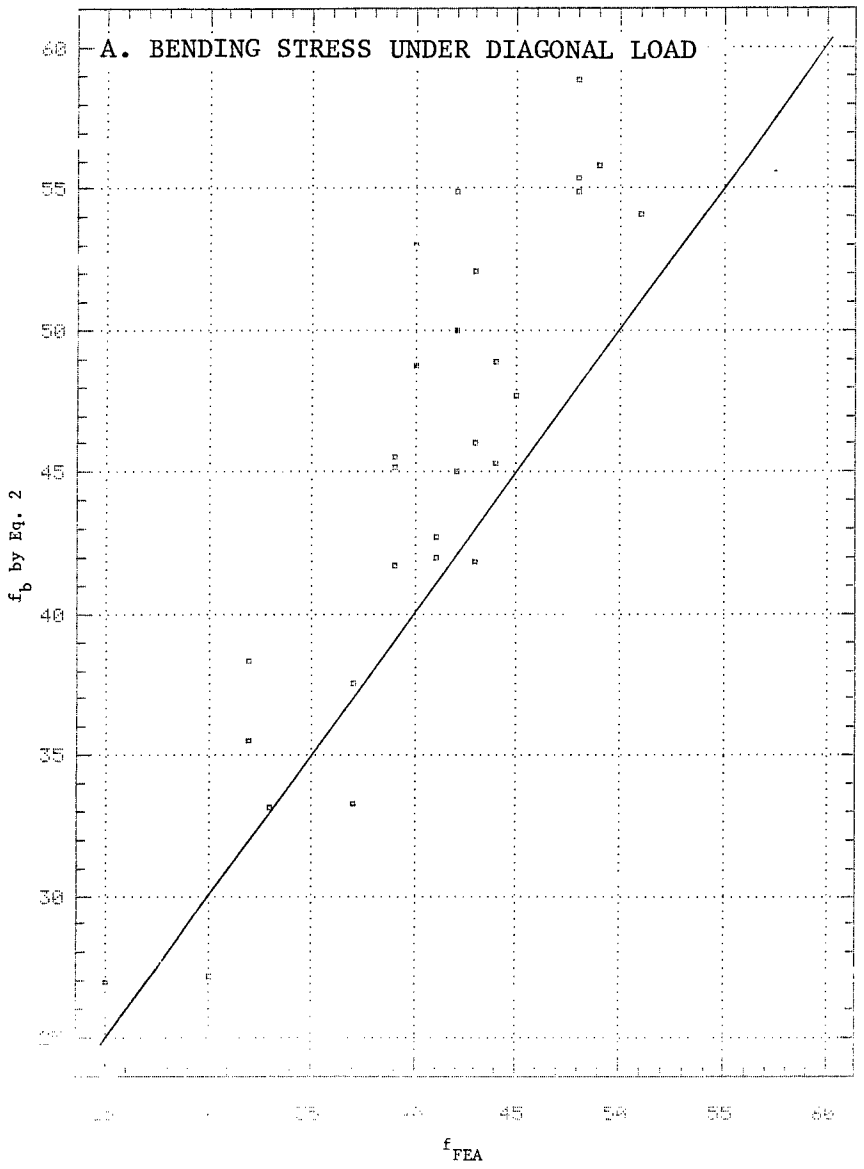

B. BENDING STRESS UNDER PARALLEL LOAD
f_b by Eq. 2
f_{FEA}
62
57
52
47
42
37
32
27

C. SHEAR STRESS UNDER PARALLEL LOAD
f_b by Eq. 2
f_{FEA}
40
36
32
28
24
20
16

Equivalent coefficient α = {4.304 - 0.02021(29/2) - 4.304(16.5/27) + ...

+ 4.503(16.5/27)^2 - 0.9750(27-0.707(29))/(27 -16.5) - 1.686(29/27)}/1.097

= 0.5909

Equivalent section modulus = 0.5909(1.414 x 27 - 16.5)2^2/6 = 8.541(in^3).

Maximum bending stress = 75.72 x 6.25/8.541 = 55.4(ksi) > 46.2 ksi. NG.

Step 2: Increase the thickness T by 0.25 in.: L = 27 in., T = 2.25 in., BC = 29 in., and DB = 16.50 in.

For maximum bending stress under diagonal loading

Anchor force = 75.72(kips).

Moment arm = 6.25(in).

Equivalent coefficient α = {4.304 - 0.02021(29/2.25) - 4.304(16.5/27) + ...

+ 4.503(16.5/27)^2 - 0.9750(27 - 0.707(29))/(27 - 16.5) -1.686(29/27)}/1.097

= 0.6206

Equivalent section modulus = 0.6206(1.414 x 27 - 16.5)2.25^2/6 = 11.35(in^3).

Maximum bending stress = 75.72(6.25)/11.35 = 41.7(ksi) < 46.2 ksi. OK.

For maximum bending stress under parallel loading

M = 6 x (32 - 1.5) x 12 = 2196(kip-in.)

L' = max{0.707 x 29,16.5} = 20.50(in.)

DB/L' = 16.5/20.50 = 0.8049, 1 - DB/L' = 0.1951

Midspan moment = 2196/4/0.8049^2{0.25 - 0.1951/3 + 0.1951^4/12} = 156.8(kip-in.)

β = {157.6 - 21.85(27/16.5) - 0.3300(29/2.25) - 259.3(16.5/27) - ...
- 48.13[(27)(2.25)/16.5/(27 - 16.5)]$^{1/2}$ + 194.6(16.5/27)^2 + 127.4
(2.25/29) - 21.65(16.5/29)}/1.080 = 0.8070

Equivalent section modulus = 0.8070(29 - 16.5) x 2.25^2/12 = 4.256(in^3)

Maximum bending stress = 156.8/4.256 = 36.84(ksi) < 46.2 ksi

For maximum shear stress under parallel loading

M/2 = 6 x (32 - 1.5) x 12/2 = 1098(kip-in.)

$b = \min(0.707 \times 29, 16.5) = 16.5(\text{in.})$

$b/T = 7.333$, $C' = 0.301$

$\gamma = (210.0 - 66.9(29/16.5) - 0.1719(29 - 16.5)/2.25 - 714.8(16.5/27) + \ldots$

$+ 358.3(16.5/27)^2 - 48.16(27 - 0.707(29))/(27 - 16.5) - 288.2(29 - \ldots$

$- 16.5)/(1.414(27) - 16.5) + 381.0(29/27))/1.094 = 1.545$

Equivalent torsional section modulus $= 1.545(0.301)16.5(2.25^2) =$

$38.85(\text{in.}^3)$

Maximum shear stress $= 1098/38.85 = 28.28(\text{ksi}) \approx 28$ ksi. OK.

Based on experience with several such redesign examples for deficient existing poles, increasing the base plate thickness is found to be most effective in reducing stress levels in the base plate.

V. CONCLUSIONS AND RECOMMENDATIONS

1. Materials and load testing, as well as FEA, show that some existing signal poles in New York are to some degree structurally inadequate, with respect to the strength requirement governed by the design load according to the current code (2). Possibly deficient components are the base plate, anchor bolts, and hand hole reinforcement. The post is found to be adequate.

2. Both diagonal and parallel loading cases. Generally, both should be included in designing signal poles.

3. Diagonal load should be used as the critical case for anchor bolt design. It is recommended that the space between the base plate and foundation be removed as soon as possible after erection to significantly reduce or eliminate bending stress in the anchor bolts. This bending was observed, but is not addressed in the current design method.

4. The current design methods for the post and hand hole appear to be appropriate. It is recommended that during erection the span wire be placed in a direction parallel to the plane of the hand hole (Case I in Fig. 20), to reduce the probability of exposure to high stresses.

5. A semi-empirical design method is suggested for the base plate, treating it as three individual simple components for corresponding critical stress cases under the two critical loading cases. This method presents clear mechanical origins of stress concentration in a simple manner. Hand calculation is sufficient for its design applications. It can also be computerized for routine practice.

6. The fact that some existing poles proved to be deficient (in some components) with no reported incident of catastrophic structural failure shows that these poles actually may not have been exposed to their design loads. Investigation may be worthwhile to collect data on their service loads.

ACKNOWLEDGEMENTS

Dr. Deniz Sandhu of the Engineering Research and Development Bureau conducted the statistical analysis in this study. Larry N. Johanson of the Structures Division worked closely with the research staff throughout this study. Cooperation of Graham Scaife and the staff of the Carlan Manufacturing Company for load testing is gratefully acknowledged. Load testing was assisted by Everett W. Dillon and Wilfred J. Deschamps of the Engineering Research and Development Bureau, and David M. Berkley from the Structures Division. Michael J. Gray of the Construction Division provided valuable recommendations to refine the FEA computer model, and Jyotirmay Lall of the Engineering Research and Development Bureau assisted in preparing the examples and part of the FEA. George L. Howard and the staff of the Materials Bureau tested the material samples. Idris A. Aziz, Everett W. Dillon, and Donna L. Noonan of the Engineering Research and Development Bureau assisted in preparing the figures.

REFERENCES

1. "Method for Calculating the Loads Applied to Span Wire Traffic Signal Poles." Engineering Instruction 83-38, New York State Department of Transportation, Sept. 14, 1983.

2. "Standard Specifications for Structural Supports for Highway Signs, Luminaries and Traffic Signals." Washington: American Association of State Highway and Transportation Officials, 1985.

3. CASA/GIFTS User's Reference Manual. Software Package Version 6.4.3. Oct. 1989

4. R. A. Cook, G. T. Doerr, and R. E. Klingner. Design Guide for Steel-to-Concrete Connections. Research Report 1126-4F(FHWA/TX-89+1126-4F), Center for Transportation Research, Bureau of Engineering Research, the University of Texas at Austin, March 1990.

5. F. P. Beer and E. R. Johnston. Mechanics of Materials. New York: McGraw-Hill Book Company, 1981.

APPENDIX A. LOADING JACK DETAILS

Provided by Carlan Manufacturing Inc., Long Island, NY

Serial No.	222
Capacity	10,000 psi
Piston Area	2.236 sq in.
Max. Stroke	14 in.
Accuracy	± 1% of full scale
Manufacturer	WB Equipment Service Co., Inc.
	Mount Vernon, N.Y.

NOTE: The zero reading of the gage dial was set at 400 psi. Accordingly, recorded gage readings were calibrated by subtracting 400 psi from each reading. Applied forces were obtained by multiplying the gage readings by the piston area.

APPENDIX B. TECHNICAL DETAILS OF STRAIN GAGES USED

All the electrical resistance gages used were manufactured by Measurements Group Inc. Two types of single-arm self-temperature compensating strain gages measured the axial stresses/strains in the base plate and the pole: 1) CEA-06-125UN-350 with a gage factor of 2.09, and 2) CEA-06-250BF-350 with a gage factor of 2.055. The strain measured from these gages is given by

$$\epsilon = 4.0 * V_{out} / (GF * V_{excit)} \text{ and } \sigma = E * \epsilon$$

where ϵ = strain, E = elastic modulus of steel = 29,000 ksi, V_{out} = output voltage, V_{excit} = excitation voltage, GF = gage factor, and σ = stress.

Three-arm self-temperature compensating rectangular rosettes of Type CEA-06-250UR-350 were used at some locations on the base plate. Gage factors for Arms 1, 2, and 3 (numbered counterclockwise) were 2.085, 2.095, and 2.085 respectively. For simplicity and ease of calculations, a gage factor of 2.09 was used for all arms. Strain corresponding to each arm was calculated in the same manner as to single arm gages explained above. Once strains corresponding to each arm $\epsilon 1$, $\epsilon 2$, $\epsilon 3$ were found, principal strains ($\epsilon_{p,q}$) and stresses ($\sigma_{p,q}$) can be calculated as follows:

$$\epsilon_{p,q} = 0.5 \left[\epsilon 1 + \epsilon 3 \pm \sqrt{(\epsilon 1 - \epsilon 3)^2 + (2\epsilon 2 - \epsilon 1 - \epsilon 3)^2} \right]$$

$$\sigma_{p,q} = 0.5 \left[\frac{\epsilon 1 + \epsilon 3}{1 - \mu} \pm \frac{1}{1 + \mu} \sqrt{(\epsilon 1 - \epsilon 3)^2 + (2\epsilon 2 - \epsilon 1 - \epsilon 3)^2} \right]$$